Eur. J. Mineral., 37, 555–576, 2025
https://doi.org/10.5194/ejm-37-555-2025

European Journal of Mineralogy
Open Access

Natrolitised nepheline-bearing Teschenite Association rocks from the Podbeskydí area (Czech Republic): a testimony from selected accessory minerals

Dalibor Matýsek[1], **Jakub Jirásek**[2], **Štěpán Chládek**[1], **and Ondřej Pour**[2,3]

[1]Department of Geological Engineering, VŠB-Technical University of Ostrava, Ostrava, 70800, Czech Republic
[2]Department of Geology, Palacký University in Olomouc, Olomouc, 77146, Czech Republic
[3]Czech Geological Survey, Prague, 11821, Czech Republic

Correspondence: Jakub Jirásek (jakub.jirasek@upol.cz)

Received: 12 September 2024 – Revised: 15 May 2025 – Accepted: 16 May 2025 – Published: 19 August 2025

Abstract. Only a few natrolitised Teschenite Association rock bodies of Early Cretaceous age from northeast Czech Republic are known. They belong to numerous small volcanic bodies within the nappes of the outer Western Carpathians. Due to the proven presence of nepheline, we can anticipate that the original rocks were nepheline-bearing igneous rocks – nephelinolites such as melteigites or ijolites. From the various accessory minerals, our research focused on several Sr-, Nb-, Ti-, and rare earth element (REE)-bearing phases. Loparite forms polygonal anhedral grains and rarely also cubic habits. The majority of the 29 spots measured correspond to niobian–calcian loparite in the lueshite–perovskite–loparite classification diagram; only two analyses fall in the ceroan–calcian lueshite field. Loparite grains are rarely accompanied by uncertain Ca–LREEs–titanoniobate (where LREEs denotes light rare earth elements). Its appearance is very similar to loparite – it forms polygonal grains clearly altered from the outer surface. Its average formula based on 11 spots can be written as $(Ca_{1.41}Sr_{0.01}LREE_{0.75}Fe^{3+}_{0.07}Al_{0.01}Th_{0.02})_{\Sigma 2.27}(Ti_{2.58}Nb_{1.58}Ta_{0.04}Si_{0.14}Zr_{0.01})_{\Sigma 4.34}(O_{11.95}F_{0.05})_{\Sigma 12.00}\cdot nH_2O$, with the ThO_2 content elevated compared to local loparite. The pyrochlore group minerals were recognised as minor to rare accessories, forming small, homogeneous, mostly unaltered grains $\leq 30\,\mu m$ in size. They correspond to an *A*-site Ca-dominant members fluorcalciopyrochlore, hydroxycalciopyrochlore, or oxycalciopyrochlore and vacancy-dominant fluorkenopyrochlore (yet unapproved by the International Mineralogical Association). Rare stronalsite forms anhedral aggregates up to 1 mm, always accompanied by the more common slawsonite. Its average formula based on 10 spots is $(Na_{1.98}K_{0.3})_{\Sigma=2.01}(Sr_{0.73}Ba_{0.14}Ca_{0.01}Fe_{0.01})_{\Sigma=0.90}Al_{3.92}Si_{4.11}O_{16.00}$. Apart from those, we also noticed the presence of Sr-rich apatite to fluorcaphite, strontiofluorite, and REE–fluorocarbonate. From the accessory phases, the natrolitisation mostly affected the primary Na–Ca feldspars through the release of sodium, barium, and strontium, transforming them into natrolite, thomsonite–Ca, celsian, stronalsite, and slawsonite. Pyrochlore group minerals show a higher degree of alteration than perovskite subgroup minerals; the temperature of such a transformation can be estimated at $\sim$ 250–150 °C based on an analogy with alkaline complexes.

1 Introduction

This paper is focused on the occurrence of selected accessory minerals – loparite, lueshite, Ca–LREE titanoniobate, pyrochlore group minerals, and stronalsite – in natrolitised Teschenite Association rocks in the Podbeskydí area (Czech Republic). The localities investigated represent strongly (auto-)metasomatised feldspathoid rocks of Early Cretaceous age in a pre-altered state close to melanocratic nephelinolites or ijolites.

For the purpose of this study, we focused on three igneous bodies: Nový Jičín–Čerťák, Brušperk–Borošín, and Bruzovice. Many accessory minerals were investigated in detail from the first site mentioned : celsian, slawsonite, and thomsonite–Ca by Matýsek and Jirásek (2016); fluorapatite, gittinsite, titanite, vesuvianite, and zircon by Kropáč et al. (2020); and allanite-(Ce), epidote, and epidote-(Sr) by Kropáč et al. (2024). However, Brušperk and Borošín were in the last decades mentioned only in one study (Rapprich et al., 2024) focusing on clinopyroxenes, where some of the accessory minerals were mentioned but without the details regarding their appearance or mineral chemistry.

The selection of accessory minerals for this study is based on (1) the lack of their previous description (loparite, lueshite, Ca–LREE titanoniobate) or missing details on their composition (pyrochlore group minerals) and (2) their potential to contribute to the understanding of the feldspathoid and plagioclase natrolitisation process.

Loparite – $(Na,REE,Sr,Ca)(Ti,Nb)_2O_6$ or ideally $(Na,REE)Ti_2O_6$ – belongs to the perovskite subgroup of stoichiometric oxide single-pyrochlore minerals and thus to the perovskite supergroup (Mitchell et al., 2017). The mineral was first described at a locality called Maly Mannepakhk Mountain in the Khibiny Massif, Murmansk, Russia (Sitnin and Leonova, 1961; Tolok and Bazhenova, 1965). The Levinson modifier was amended to the mineral name in 1987, so it has been known as "loparite-(Ce)" since then (Nickel and Mandarino, 1987). The REE content of loparite tends to be necessary for its electrostatic equilibrium, but Na is the predominant *A*-site cation in all samples that have been analysed until now. Due to this reason, the mineral was renamed loparite during the last revision of the perovskite supergroup minerals (Mitchell et al., 2017). The name loparite without the Levinson modifier is the only valid form now (Bosi et al., 2024).

Both loparite itself and the other minerals of the perovskite group are characterised by extreme isomorphic substitution in cationic positions (e.g. Mitchell and Chakhmouradian, 1996; Locock and Mitchell, 2018). Although the crystal structure of loparite is of the pyrochlore type, it is typically somewhat distorted due to substitutions (Mitchell et al., 2000). Using single-crystal diffraction, the authors found variability in the space groups *Pbnm* and *I*4/*mcm*, with no evidence of cation ordering. Popova et al. (2017) described an orthorhombic structural variety belonging to the space group *Ima*2.

The majority of the global occurrences of loparite and its chemically and structurally related minerals (tausonite, lueshite, etc.) belong to carbonatites (e.g. Haggerty and Mariano, 1983; Platt, 1994), agpaitic alkaline massifs (Kogarko et al., 2002; Konopleva et al., 2017; Chakhmouradian et al., 2007 and others), and lamproites and peralkaline pegmatites (Mitchell and Chakhmouradian, 1999). It is also known from alkaline effusive rocks, i.e. trachyte and phonolite (Amores-Casals et al., 2020; Yan et al., 2022). Among the eudialyte phonolites from the carbonatite palaeo-volcano at Kola, lueshite rather than loparite has been reported (Petrovsky et al., 2012). A somewhat unusual occurrence of loparite was noted in the mafic A-type granite (Morgenstern et al., 2019).

The pyrochlore group, with the general formula $A_2Nb_2(O,OH)_6Z$, is a relatively simple group of minerals that mostly crystallise in the isometric crystal system (space group *Fd*-3*m*). The *A* site can be occupied by Na^+, Ca^{2+}, Sr^{2+}, Pb^{2+}, Sn^{2+}, Sb^{3+}, Y^{3+}, U^{4+}, H_2O, or a vacancy (□), and the *Z* site can contain $(OH)^-$, F^-, O^-, H_2O, or a vacancy (Atencio et al., 2010). However, different classification approaches can be applied to this group (see Bhattacharjee et al., 2022). From ca. 50 possible natural end members, only 11 are considered valid minerals (Atencio et al., 2010; Christy and Atencio, 2013; Atencio, 2021). Due to its high niobium content, phases belonging to this group are typical of granitic pegmatites, alkali rocks, carbonatites, and some metasomatic rocks (overview in Yaroshevskii and Bagdasarov, 2008).

Stronalsite – $Na_2SrAl_4Si_4O_{16}$ – forms continuous isomorphic series with banalsite ($Na_2BaAl_4Si_4O_{16}$) and is relatively rare in nature (Koneva, 1996). It is known from fewer than 20 localities worldwide. Stronalsite is a tectosilicate classified in the feldspar group. However, the structural arrangement of its tectosilicate framework is quite different from that of the feldspars, and the arrangement of cations in the framework cavities is also diverse. According to the structural data (Liferovich et al., 2006a), the main differences concern the distribution of the orientations of the apical oxygen atoms (in the 001 plane), which consequently results in a different frequency of tetrahedra in their rings. Minerals of the stronalsite–banalsite series are orthorhombic, belonging to the non-centro-symmetric space group *Iba*2. Stronalsite was first described together with slawsonite and pectolite in veins in xenoliths in rodingites within a serpentinite quarry near Kochi, Japan (Hori et al., 1987). From a jade deposit, stronalsite and banalsite were reported by Ferraris et al. (2014). However, occurrences of stronalsite are mainly associated with alkaline intrusive massifs (nepheline syenite, jacupirangite, nepheline melilitite, etc.) and the mafic xenoliths within them, where their occurrence is associated with hydrothermal or metasomatic alteration (Liferovich et al., 2006b). Medvedeva et al. (2016) described banalsite–stronalsite from melanocratic feldspathoid alkali–feldspar syenites of the Mi-

askite Massif in the southern Urals and linked its formation to alkali metasomatism. Zozulya et al. (2009) reported stronalsite from a cancrinite syenite from a Late Archean alkaline massif in Norway. An interesting case of the formation of a stronalsite–banalsite-series mineral during the hydrothermal alteration of lujavrite (Pilansberg [Pilanesberg] alkaline complex, South Africa) is described by Mitchell and Liferovich (2006). Stronalsite–banalsite series minerals are also known from carbonatites (e.g. Ahijado et al., 2005; Dubina et al., 2022). Dahlgren and Larsen (2012) described them in amygdaloid cavity fills in ultramafics of Carboniferous to Permian age in the Brunlanes ultramafic series in Norway.

2 Geological setting

The Cretaceous igneous and volcanoclastic rocks studied, known as Teschenite Association rocks (hereinafter referred to as TARs), are embedded as lavas or penetrate as dikes and sills in the Early Cretaceous sedimentary sequences of the outer Carpathians (Menčík et al., 1983; Włodyka, 2010). The outer Flysch Carpathians represent the most external zone of the Carpathian mountain chain, which is part of the Alpine–Carpathian–Dinaridic orogenic system (Schmid et al., 2008) extending over southern, central, and eastern Europe. Part of this mountain chain, extending from the eastern Czech Republic to southern Poland, comprises folded and thrusted strata of latest Jurassic to Lower Miocene age (Fig. 1). All of the nappe allochthons were thrusted more than 60 km over the Miocene sediments of the Carpathian Foredeep (Picha et al., 2006).

The TARs are bound to the Silesian Nappe, which consists of predominantly flysch sediments of Late Jurassic to Oligocene origin that were deposited in the Silesian Basin (Menčík et al., 1983; Picha et al., 2006). Volcanic activity has been dated to the Early Cretaceous, as evidenced by the radiometric ages (Lucińska-Anczkiewicz et al., 2002; Szopa et al., 2014).

The TARs are characterised by highly variable mineral proportions, with forsteritic olivine, clinopyroxene, amphiboles, and K–feldspars and plagioclases as the main primary rock-forming minerals. In addition to phaneritic rock types with a gabbroic appearance, the TARs also include alkali lamprophyres and fine-grained porphyritic and aphanitic types from effusive or near-surface intrusive bodies (Dostal and Owen, 1998; Włodyka, 2010; Matýsek et al., 2018). Zeolitisation (mainly analcimisation), chloritisation, smectitisation, and carbonatisation are the most frequent alteration processes associated with this rock suite (e.g. Dolníček et al., 2010b; Matýsek et al., 2018; Matýsek and Jirásek, 2023).

3 Samples

The samples investigated came from three localities in the northeastern Czech Republic – Čerťák near Nový Jičín, Borošín near Brušperk, and Bruzovice–Pazderůvka (Table 1). Other natrolitised TAR bodies are mentioned only to supply information about their existence.

Čerťák near Nový Jičín (formerly also known as Čertův Mlýn, Teufelsmühle in German) and its surroundings have long been a well-known and widely studied locality of the rocks of the Teschenite Association in the Podbeskydí area. The locality, or rather the zone of several sub-locations, lies near the Čertův Rybník water reservoir in the western part of the cadastre of the village of Bludovice near Nový Jičín and extends into the cadastre of the village of Kojetín near Starý Jičín. The petrography and mineralogy of the area have been dealt with or at least mentioned by authors since the second half of the 19th century. More recently, the locality was studied by Matýsek and Jirásek (2016) and Kropáč et al. (2020, 2024). However, the published data on the mineralogy and petrography of the igneous rocks at this locality are scarce and partially confusing. In the locality studied, a tectonically segmented sill of coarse-grained igneous rock is exposed, and it is commonly referred to by the term "teschenite" (Fig. 2c). The vein at the site is deposited in predominantly clayey sediments of the Hradiště Formation of the Silesian Unit. The igneous body forms an elongated elevated area (with a southwest–southeast orientation), is traceable over a distance of at least 1100 m, and is now exposed in three prominent remnants of old quarries from the late 19th century and also in a series of debris flows on the slopes. The thickness of the body is difficult to estimate in tens of metres (perhaps up to 50 m), and the rock fill of the body is clearly affected by the fractional crystallisation. The bedding steeply dips towards the southeast – a number of other parallel volcanite bodies of different petrographic compositions then accrete in this direction.

Most of the interesting mineralisation at the site is bound to aplitic and pegmatitoid dikes up to 8 cm thick (Fig. 2a, b). Their phase composition is the same as the surrounding rock, but they are significantly enriched in felsic minerals (Fig. 2a, b). They might be the product of magmatic fractional crystallisation followed by hydrothermal overprinting (Kropáč et al., 2020) or filter pressing at a later stage of magmatic crystallisation (Pacák, 1926; also the opinion of the authors of this article). Bulk-rock geochemical analyses of leucocratic dikes showed high alkali metal content (5.10 wt % Na_2O, 3.77 wt % K_2O; Rapprich et al., 2024).

In the vicinity of Brušperk–Borošín, a large tectonic fragment of the Silesian Unit from the area east and southeast of the town is present. This fragment is mainly composed of the lower part of the sedimentary sequence of this unit (the Hradiště Formation with layers of Těšín Limestone) and also contains numerous bodies of TAR volcanites with a variable petrographic composition. The volcanites in the

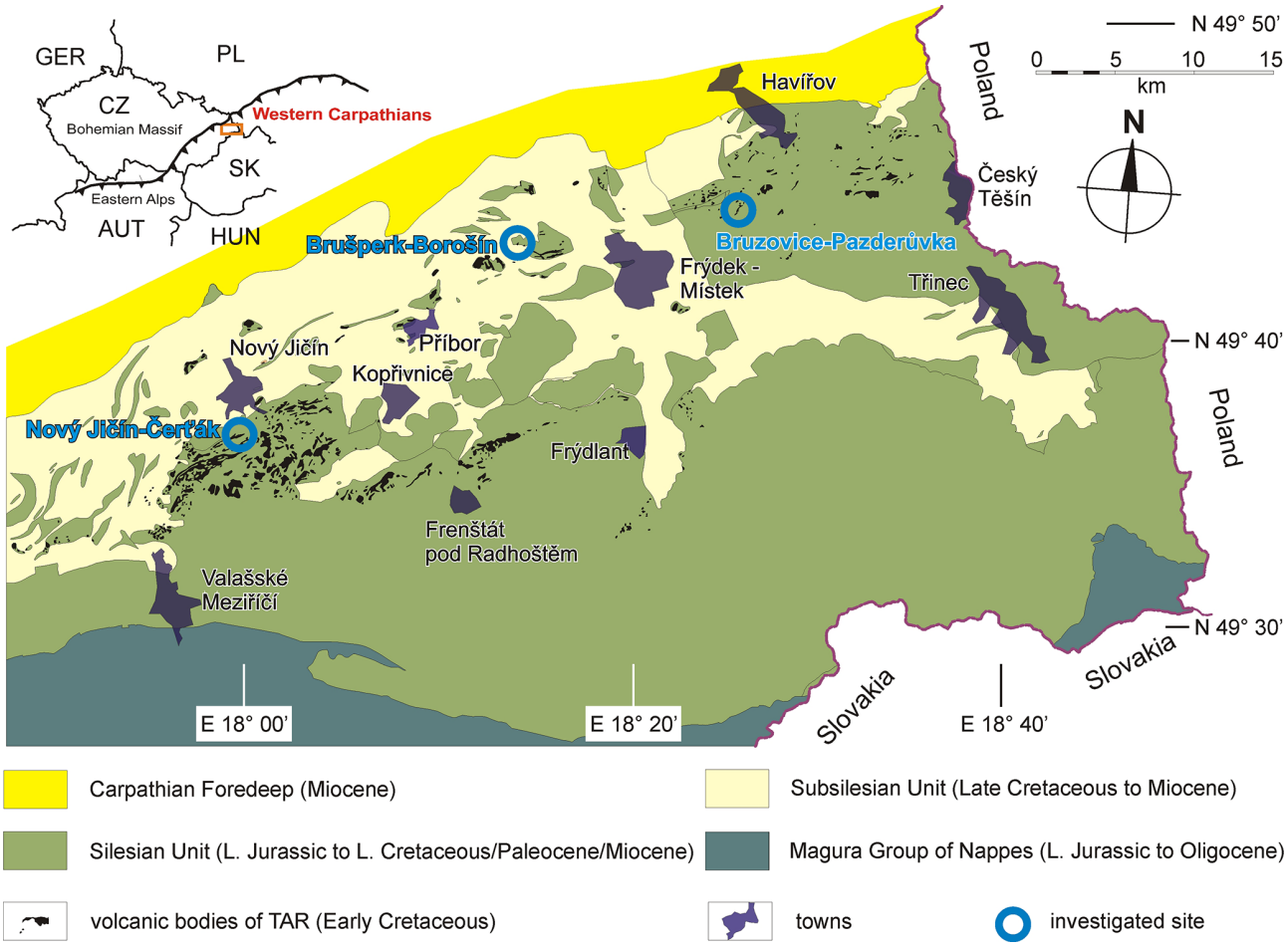

Figure 1. Schematic geological map showing the Czech part of the Podbeskydí region with the positions of the study localities (white circles). The TARs form numerous (> 1000) bodies bound to the Silesian Unit; smaller ones are not depicted on this map due to their size (modified from Matýsek and Jirásek, 2023).

southern vicinity of Brušperk correspond visually to typical teschenites (Fig. 2d), as well as to various types of picrites and to rocks traditionally referred to as monchiquites or fourchites. This locality was also mentioned in older papers (Klvaňa, 1897; Pacák, 1926), when it was an outcrop in the cut of a dirt road. However, according to aerial photographs of the area, it was ploughed up in the 1950s, and the site was forgotten. Today, it is possible to collect only locally abundant rock fragments in the field. The most interesting area is a body of coarse-grained volcanics traditionally classified as teschinites; it was labelled as Borošín 1 (see Table 1). Another body of similar composition is located ∼ 450 m away in the eastern direction (Borošín 2). The site Borošín 3 represents fragments of fine-grained volcanites of a somewhat different mineralogical composition and structure, believed to represent chilled material from the margins of the body of Borošín 1.

Pacák (1926) is the only author who has dealt with the site in Borošín in detail in the past. From the outcrop near the previously mentioned dirt road, he described medium- to coarse-grained rock with about 50 % mafic minerals. These are mainly represented by Ti-rich augite with younger aegirine. The groundmass is, according to this author, composed of fibrous zeolites, occasionally with hematite pigment and, more rarely, anorthoclase crystals. He also mentioned occasional small "concretionary" formations composed of pure fibrous natrolite (Fig. 2d). Pacák (1926) noticed that the outcrop belongs to the most alkaline rock types of the teschinite association, while all nephelines are in fact pseudo-morphed by zeolites with prevailing natrolite. Rapprich et al. (2024) published a detailed description of local aegirine and a bulk-rock geochemical analysis (6.14 wt % Na_2O, 0.45 wt % K_2O), and classified the local rock as natrolitised essexite (foid gabbro).

The Bruzovice outcrop lies on the left bank of Pazderůvka Creek. It was not noticed by previous authors. Šmíd (1978) mentioned only "diabase" from this site, but there are several small bodies of different volcanic rocks nearby. Our samples came from the one traditionally called pyroxene teschen-

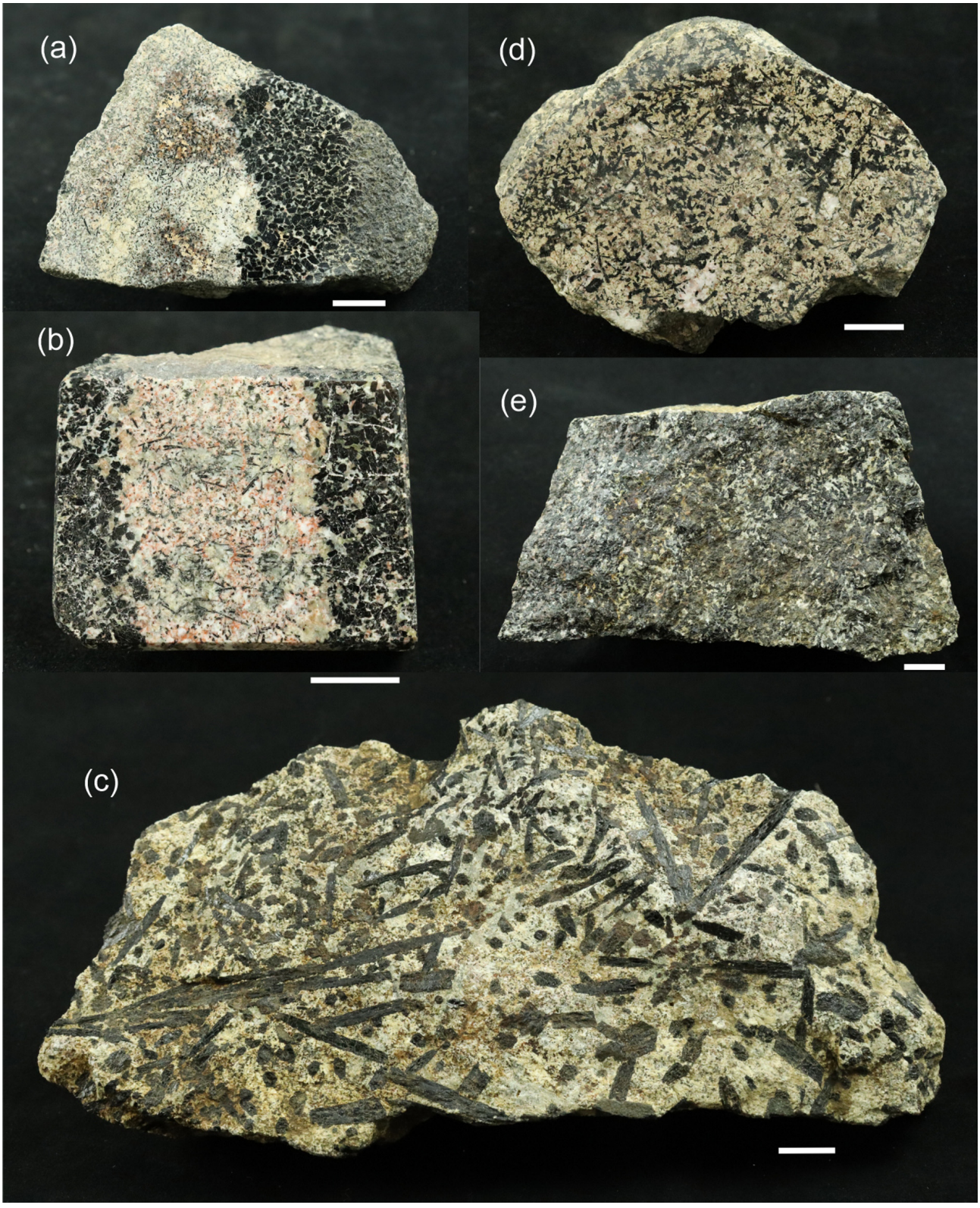

Figure 2. Typical rock samples from the localities studied: **(a, b)** leucocratic aplite to pegmatite dikes in the mafic "teschenite" from Nový Jičín–Čerťák; **(c)** coarse-grained zeolitised "teschenite" from Nový Jičín–Čerťák; **(d)** natrolitised "teschenite" from the Brušperk–Borošín site no. 1, with white spots of pure natrolite; and **(e)** natrolitised pyroxene "teschenite" from Bruzovice–Pazderůvka. The size of each sample is given by the adjacent 1 cm white line.

Table 1. Overview of the known natrolitised TARs (originally essexites to ijolites) described in detail in the text. Note that essential minerals are arranged according to their content, and accessory minerals are in alphabetical order.

Locality	GPS coordinates	Essential minerals (primary in bold)	Accessory minerals
Nový Jičín–Čerťák	49°34.187′ N 018°00.487′ E Leucocratic dikes surrounding rock	Natrolite 31 %–91 %, **diopside 2 %–24 %**, thomsonite-Ca 8 %–18 %, muscovite 2 %–29 %, **amphibole 1–6 %**, chlorite 1 %–5 %, prehnite 0 %–13 %, microcline 0 %–16 %, sanidine 0 %–13 %, orthoclase 0 %–10 %, analcime 0 %–7 %, nepheline 0 %–4 %	Allanite-(Ce)[e], baryte[d], calcite[d], celsian[c], chamosite[d], epidote-(Sr)[e], fluorapatite[d], fluorcalciopyrochlore[d], gittinsite[d], grossular[d], hedenbergite[c,d], magnetite[d], microcline[c], pyrite[d], pyrochlore group mineral (*A*-site Ca-dominant F at 0.38–1.05 apfu)[a], slawsonite[c], stronalsite[a,f], titanite[d], vesuvianite[d], zircon[d]
		Amphibole 50 %, natrolite 24 %, microcline 16 %, quartz 6 %, chlorite 4 %	
Brušperk–Borošín 1	49°41.537′ N 18°14.339′ E	Natrolite 50 %–60 %, **diopside 11 %–23 %**, orthoclase 8 %–11 %, kaolinite 5 %–6 %, aegirine 3 %–5 %, **annite 3 %–4 %**	Aegirine[f], aegirine-augite[f], analcime[f], anatase, Ca-LREE- titanoniobate[a], chalcopyrite, chlorite, fluorapatite, pyrochlore group mineral (*A*-site zero-valence dominant F at 0.65–0.81 apfu)[a], kaolinite[f], loparite[a], lueshite[a], magnetite, pyrite, titanite, titanomaghemite, slawsonite, sphalerite
Brušperk–Borošín 2	49°41.525′ N 18°14.718′ E	**Diopside 30 %–50 %**, orthoclase 16 %–18 %, chlorite 11 %–12 %, natrolite 9 %–12 %, montmorillonite 0 %–9 %, calcite 0 %–8 %, **apatite 2 %–4 %**, annite 3 %, **magnetite 3 %**, **amphibole 1–2 %**, anatase 2 %	Monazite, zircon
Brušperk–Borošín 3[b]	49°41.736′ N 18°14.393′ E	**Diopside 40 %–60 %**, chlorite 16 %–30 %, analcime 8 %–10 %, **nepheline 0 %–6 %**, orthoclase 0 %–7 %, calcite 4 %, **apatite 4 %**	Aegirine, aegirine-augite, annite, baryte, celsian, cerianite-(Ce), chalcopyrite, chlorite, fluorcaphite?, K-feldspar, kaolinite, magnetite, monazite, pyrite, rhabdophane-(La), sphalerite, strontiofluorite[a]
Bruzovice	49°43.547′ N 18°25.904′ E	Analcime 34 %, natrolite 24 %, microcline 17 %, **amphibole 16 %**, **apatite 3 %**, **biotite 3 %**, chlorite 3 %	Annite, chalcopyrite, La,Ce-fluorocarbonate, loparite[a], magnetite, monazite-(Ce), pyrite, pyrochlore group mineral (*A*-site Ca-dominant F at 0.44–1.00 apfu)[a]

[a] Newly described minerals. [b] Borošín 3 is not natrolitised but represents the chilled margin of the Borošín 1 and 2 bodies. Mineral composition ranges are based on the following number of quantitative powder X-ray analyses: Nový Jičín–Čerťák: 16 samples; Brušperk–Borošín 1: 4 samples; Brušperk–Borošín 2: 3 samples; Brušperk–Borošín 3: 3 samples; and Bruzovice: 1 sample. References to previously mentioned accessory phases are [c] Matýsek and Jirásek (2016), [d] Kropáč et al. (2020), [e] Kropáč et al. (2024), [f] Rapprich et al. (2024), and [g] Kropáč et al. (2025) – the last work was published online during the review of this paper.

ite – coarse-grained rock with a porphyritic texture of elongated black clinopyroxene phenocrysts within a white zeolite matrix (Fig. 2e). Bulk-rock geochemical analyses of the rock showed elevated alkali metal content (3.21 wt % Na_2O, 0.75 wt % K_2O; Rapprich et al., 2024).

The following numbers of analysed samples were used for the purposes of this study:

– *Nový Jičín–Čerťák*. Leucocratic aplitic and pegmatitoid dikes and the teschenite host rock: 16 quantitative powder X-ray diffractions (PXRDs), 47 polished sections

- *Brušperk–Borošín 1*. Teschenite rock: 4 quantitative PXRDs, 15 polished sections.
- *Brušperk–Borošín 2*. Teschenite rock: 3 quantitative PXRDs, 3 polished sections.
- *Brušperk–Borošín 3*. Teschenite rock: 3 quantitative PXRDs, 31 polished sections.
- *Bruzovice*. Teschenite rock: 1 quantitative PXRD, 6 polished sections.

4 Methods

The phase compositions of the samples were investigated by powder X-ray diffraction using a Bruker-AXS D8 Advance instrument (VŠB-Technical University of Ostrava, analyst Dalibor Matýsek) with a $2\theta/\theta$ measurement geometry and a position-sensitive detector (LynxEye) under the following conditions: radiation with a Cu$K\alpha$/Ni filter, current of 40 kV, voltage of 40 mA, step mode with a step size of 0.014° 2θ, and a counting time of 4 s per step.

Qualitative analysis of diffraction patterns was performed using the EVA software (Bruker-AXS) and the database PDF-2, release 2011 (International Centre for Diffraction Data). The Rietveld method using the TOPAS software version 5 (Bruker-AXS) was applied to verify the qualitative analyses and to quantify the mineral phases present. The input structural models of rock-forming minerals were taken from the Bruker-AXS Crystal Structure Database and from the American Mineralogist Crystal Structure Database and were modified based on the results of electron microanalyses.

The microchemical analyses of the perovskite subgroup minerals, pyrochlore group minerals, Ca–LREE–titanoniobate, and REE–fluorocarbonate were performed using wavelength dispersive X-ray spectroscopy (WDS) with an electron microprobe (CAMECA SX100, analyst Jakub Haifler) at the Laboratory of Electron Microscopy and Microanalysis of the Faculty of Science at Masaryk University in Brno. The standards used were almandine (Si$K\alpha$, Al$K\alpha$, Fe$K\alpha$), Mg_2SiO_4 (Mg$K\alpha$), albite (Na$K\alpha$), sanidine (K$K\alpha$), hematite (Fe$K\alpha$), Mn_2SiO_4 (Mn$K\alpha$), fluorapatite (P$K\alpha$, Ca$K\alpha$), baryte (Ba$L\alpha$), $SrSO_4$ (Sr$L\alpha$, S$K\alpha$), alamosite (Pb$M\alpha$), Bi (Bi$M\beta$), gahnite (Zn$K\alpha$), lammerite (As$L\alpha$), titanite (Ti$K\alpha$), Sn (Sn$L\alpha$), U (U$M\beta$), ThO_2 (Th$M\alpha$), zircon (Zr$L\alpha$), topaz (F$K\alpha$), vanadinite (Cl$K\alpha$), columbite (Nb$L\alpha$), $CrTa_2O_6$ (Ta$L\alpha$), scheelite (W$L\alpha$), $ScVO_4$ (Sc$K\alpha$), YAG (Y$L\alpha$), $LaPO_4$ (La$L\alpha$), $CePO_4$ (Ce$L\alpha$), $PrPO_4$ (Pr$L\beta$), $NdPO_4$ (Nd$L\beta$), $SmPO_4$ (Sm$L\beta$), $EuPO_4$ (Eu$L\beta$), $GdPO_4$ (Gd$L\beta$), $TbPO_4$ (Tb$L\alpha$), $DyPO_4$ (Dy$L\beta$), $HoPO_4$ (Ho$L\beta$), $ErPO_4$ (Er$L\alpha$), $TmPO_4$ (Tm$L\alpha$), $YbPO_4$ (Yb$L\alpha$), and $LuPO_4$ (Lu$M\beta$). The measuring conditions were 15 kV, 6 nA, and a spot size of $<$ 3 µm (perovskite subgroup, pyrochlore group, belyankinite-related phase) and 2 nA and a spot size of $<$ 8 µm (REE–fluorocarbonates).

The microchemical analyses of the stronalsite were, for the sake of more precise analysis of light elemental sodium, performed using energy dispersive X-ray spectroscopy (EDS Ultim Max 100, Oxford Instruments) coupled with an electron microscope (Tescan Mira3 GMU, analyst Ondřej Pour) at the Laboratory of Electron Microscopy and Microanalysis of the Czech Geological Survey. The standards used were almandine (Fe$K\alpha$), quartz (Si$K\alpha$), forsterite (Mg$K\alpha$), albite (Na$K\alpha$), orthoclase (K$K\alpha$), plagioclase (Ca$K\alpha$, Al$K\alpha$), rhodonite (Mn$K\alpha$), celestine (Sr$L\alpha$), fluorapatite (P$K\alpha$), rutile (Ti$K\alpha$), baryte (Ba$L\alpha$), and topaz (F$K\alpha$). The analyses were conducted with an accelerating voltage of 15 kV, an absorbed current of $\sim$ 3 nA, a spot size of $<$ 8 µm, and a working distance of 15 mm. Counting times were 10 s. Analyses were processed with the Aztec 6.0 software.

The samples' microstructures were investigated by analysing the natural rock fracture surfaces, polished sections, and also polished sections following the removal of the carbonate component by etching in a sodium–acetate buffer using an auto-emission electron microscope called the FEI Quanta-650 FEG from FEI (now Thermo Fisher Scientific Inc.). Photomicrographs were obtained using a backscattered electron (BSE) detector in chemical gradient mode.

The empirical formulae of the loparite and lueshite were calculated based on Locock and Mitchell (2018) and the pyrochlore formula following Atencio et al. (2010). The composition of the natrolite framework tetrahedra is expressed by the ratio Tsi = Si/(Si + Al), according to Tschernich (1992).

5 Results

5.1 Petrography of natrolitised rocks

5.1.1 Nový Jičín–Čerťák locality

From the Nový Jičín–Čerťák locality, more than 40 rock samples of leucocratic aplitic and pegmatitoid dikes (Fig. 2a) and the host rock were investigated. In this text, we report only new findings since the locality has been described in several recent works (Matýsek and Jirásek, 2016; Kropáč et al., 2020, 2024). Despite the original assumption of rare accessory minerals occurring only in the leucocratic aplitic and pegmatitoid dikes, we have found slawsonite, banalsite, pyrochlore group minerals, and other accessories directly situated in the various rock types, including melanocratic ones. The only difference is the share of the felsic minerals, which in fact results in easier finds of rare minerals in the leucocratic dikes, where they are not "diluted" by clinopyroxene and amphibole.

The leucocrate part of the mafic rocks and the matrix of the leucocratic dikes are formed by a micaceous illite–paragonite phase (Fig. 3a), a fine-grained mixture of natrolite with Sr-rich thomsonite-(Ca) (Fig. 3b–d), Ba-rich K and Na–

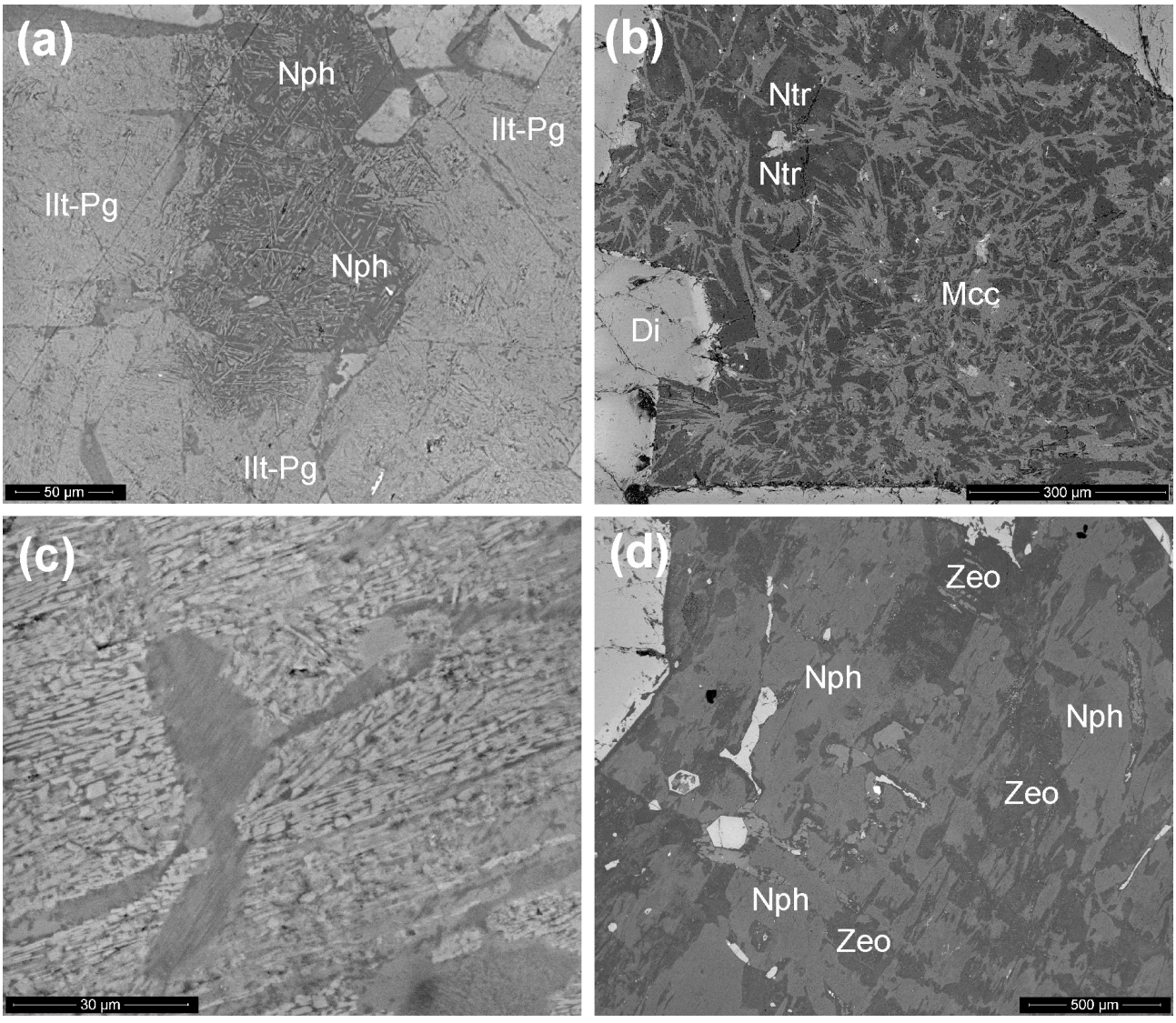

Figure 3. BSE images of the leucocratic dikes from the Nový Jičín–Čerťák locality: **(a)** illite–paragonite (Ilt–Pg) partial pseudomorph after nephelinite (Nph), **(b)** non-fibrous natrolite (Ntr) filling spaces between subhedral microcline laths (Mcc), **(c)** detailed view of the natrolite–thomsonite-(Ca) rock matrix, and **(d)** nepheline (Nph) partially altered to a mixture of zeolites (Zeo).

K feldspars (Fig. 3b), and prehnite. Alkali feldspars (Fig. 3b) almost always show a higher degree of euhedral confinement than the other components, with the exception of mafic minerals. The texture is ophitic. Relics of albite occur only rarely in the set of samples studied (although it is reported as abundant by Kropáč et al., 2020) and form only locally developed polygonal patches within the potassium feldspar lamellae.

Natrolite is certainly a more abundant component of the leucocratic component of the rocks than analcime is. The latter, similar to prehnite, occurs locally (Table 1). Both minerals usually fill cavities and the polygonal spaces between the subhedral laths of potassium feldspar (Fig. 3b). Natrolite is also apparently only locally fibrous; its fibres are commonly of sub-micrometre thickness (Fig. 3c), which may greatly affect its identification by optical methods. Thomsonite is commonly embedded in the natrolite groundmass in the form of fibrous patches (Fig. 3c). The fibrous structure of the natrolite groundmass was revealed by etching (e.g. in acetic acid).

Another interesting feature is the finding of a few grains of relatively well-preserved nepheline. This forms anhedral grains between the potassium feldspar laths that are densely intergrown with very fine flakes of micaceous mineral (Fig. 3a) or euhedral-to-subhedral crystals altered to zeolites (Fig. 3d). The identification of nepheline is based only on semi-quantitative EDS microanalyses (the grain shows atomic ratios of Si = Al and Na/K of ~ 3). Equally exceptional is the finding of a relatively well-preserved plagioclase

forming two subhedral grains strongly analcimised from the margins.

5.1.2 Brušperk–Borošín locality

Samples from the Brušperk–Borošín locality came from three distinct sites. Site no. 1 corresponds macroscopically to typical pyroxenic tephrites. The proportion of pyroxenes to groundmass is quite variable, indicating the differentiation of the body. Columnar pyroxenes up to 1.5 cm in length are the only phase recognisable to the naked eye (Fig. 2b). They are embedded in a fine-grained, light beige or greenish groundmass, occasionally containing white spots. Unfilled miaroles are relatively abundant. The results of powder X-ray diffraction analyses showed that natrolite and pyroxene close to diopside are the dominant components of the rock. The proportion of natrolite, according to Rietveld analysis, ranges from 46 wt % to 60 wt %, and the white patches in the rock correspond to almost pure natrolite. The lattice parameters of natrolite are in agreement with the published data for natrolite (see Table S1 in the Supplement). Analcime was found only very rarely and only in trace amounts; the rock samples studied do not contain plagioclase at all, not even albite. In addition, potassium and sodium feldspar (up to 10 wt %, with diffraction corresponding to Na–orthoclase), apatite, a mica mineral (probably annite), and aegirine clinopyroxene were observed. Weathering products (chlorite, kaolinite, possibly anatase) are abundant. It is possible to interpret natrolite pseudo-morphoses after nepheline in the groundmass due to the poorly constrained rectangular cross-section shapes in a number of samples. The magnetic concentrate obtained using the permanent magnet from the ground rock contains at least two oxyspinel phases (magnetite, titanomaghemite), as well as titanite and anatase. This composition is indicative of the significant and polygenetic alteration of Ti–Fe oxides.

Using electron microscopy and microanalysis, it was found that natrolite forms completely anhedral masses. It is micro- to nano-crystalline and encloses unusually abundant inclusions and crystals of other minerals. The fibrous structure of natrolite is only observable after etching (e.g. with acetic acid; Fig. 4a), with fibre thicknesses in the hundreds of nanometres. WDS microanalyses of the natrolite (Table S4) display only minor deviations from the theoretical composition, consisting of a very slight excess of Si over Al in the zeolite framework. The substitution of Na^+ with other cations in the extra framework positions is insignificant.

The natrolitic groundmass contains mainly euhedral crystals of diopside and euhedral radial needles of aegirine (Fig. 4a, b). Diopside is frequently zoned with rims and overgrowths of aegirine–augite to aegirine. Chlorite particles in the matrix are widespread. The potassium feldspar forms lath-shaped crystals in the groundmass. In addition, anhedral inclusions of various minerals with a maximum size of 50 µm have been found in natrolite. In particular, celsian is abundant in the form of polygonal grains. Two different phases belonging to the perovskite subgroup; a mineral of the pyrochlore group (see Sect. 5.2); a Ce-dominated REE–phosphate (probably monazite); pyrite, including its alteration products; chalcopyrite; a phase close to CuS; sphalerite; and others were found. Euhedral apatite is enclosed in both clinopyroxenes and the natrolitic matrix, where it also has thin outer rims (about 5 µm) of an Sr-rich mineral (Sr-rich fluorapatite or fluorcaphite; Fig. 4c, d).

In the miarole walls, phases formed by weathering (Mn and Fe–oxides, kaolinite, cerianite-(Ce), rhabdophane-(La), baryte, etc.) have been detected, in addition to aggregates of natrolite crystals and abundant euhedral apatite, including Sr-rich apatite and/or fluorcaphite coatings, aegirine, and celsian. The Sr-rich variety of apatite or possibly fluorcaphite, reported from the Teschenite Association rocks by Kropáč et al. (2017), could not be reliably analysed due to its small size. Our EDS analyses yielded an average of 16.17 wt % SrO and an atomic ratio of $Sr/(Sr + Ca) = 0.18$, which is high enough for fluorcaphite, but without a reliable determination of the cationic arrangement in the individual structure sites, its identification is still only hypothetical. Quite exceptionally, according to EDS microanalyses, 5 µm inclusions have also been found in natrolite, with a SrF_2 (strontiofluorite) composition (Figs. S1 and S2 in the Supplement). We identified slawsonite – an Sr-rich phase belonging to the feldspar group – only once, at the outskirts of site no. 1. It forms pseudomorphs after the unidentified phase, accompanied by the mineral mica (Fig. 4e).

Alterations of Ti–Fe oxides, originally Ti-rich magnetite, occur as partial-to-complete pseudo-morphoses ("leucoxene" sensu lato). These pseudo-morphoses are extremely heterogeneous and are densely fractured (Fig. 4e). Pseudomorphoses after Ti–Fe oxides are regularly lined with a coating composed of crystals of a high-Fe, low-Al annitic mica. It is probably formed by reactions between the natrolite groundmass and Ti–Fe oxides during post-volcanic alteration processes.

The rocks from the Brušperk–Borošín site no. 2 are characterised by numerous features that are similar to the previous site, no. 1, but they are mesocratic instead of leucocratic. The natrolite content is also the dominant component of the groundmass (see Table 1), and plagioclase is also completely absent. There is a much lower proportion of accessory minerals; only zircon and monazite have occasionally been found.

At the Brušperk–Borošín site no. 3, rounded fragments of fine-grained rock with a basaltic appearance occur. This site is particularly important with respect to the interpretation of the formation of the local Teschenite Association rocks and their alteration, as partially preserved nepheline was found quite abundantly in the samples. Powder X-ray diffraction analyses showed that chloritised pyroxenic rock contains variable amounts (max. 10 %) of nepheline and analcime. In addition, the rock contains apatite; the mineral mica; calcite; kaolinite; and, in some samples, potassium feldspar. Using SEM/EDS, nepheline was found to form subhedral grains

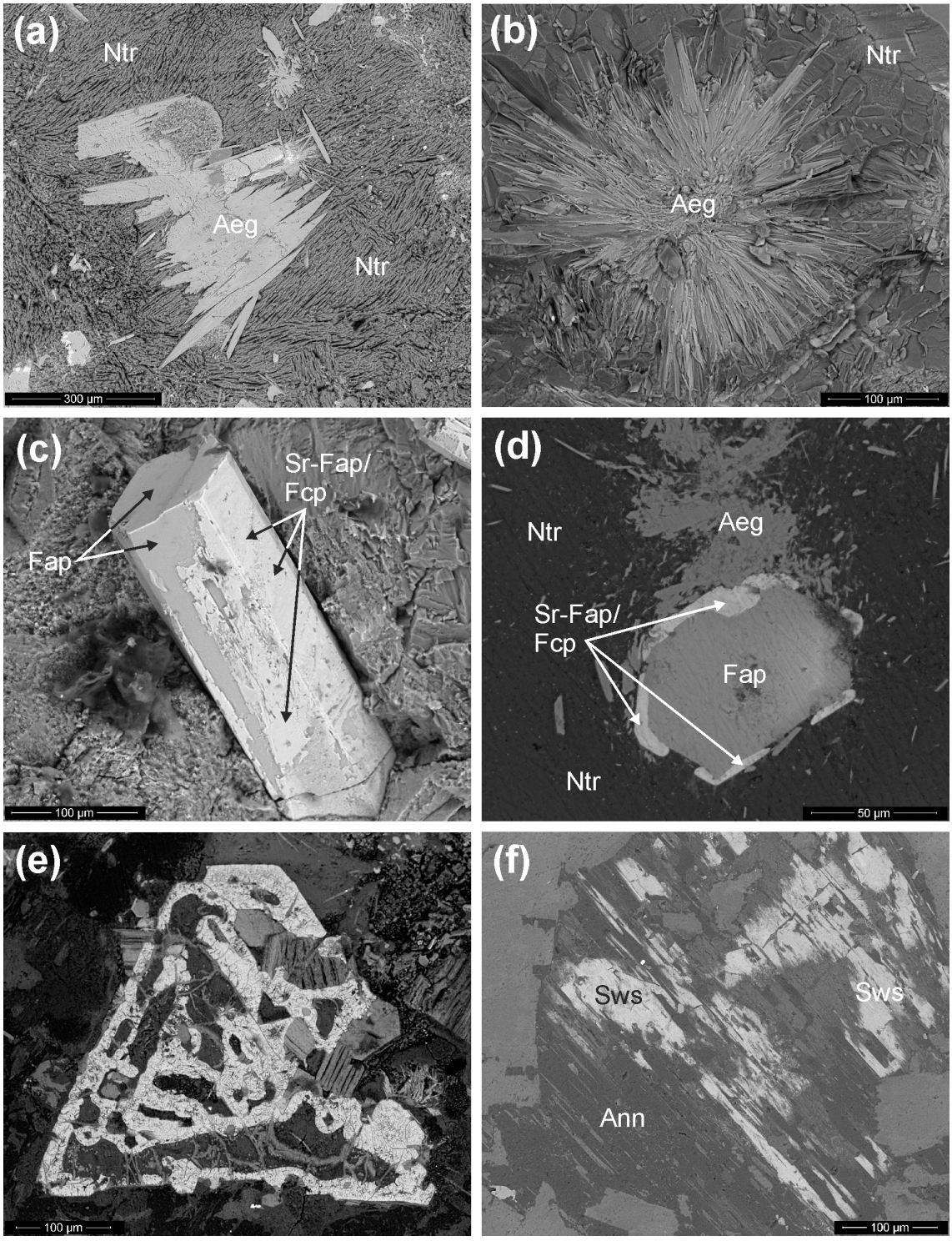

Figure 4. BSE images of the minerals from the Brušperk–Boroš́in site no. 1. **(a)** acicular aegirine (Aeg) in the natrolite (Ntr) matrix. The natrolite texture was emphasised by etching in acetic acid. **(b)** Radial aegirine (Aeg) aggregate on the natural fracture of the natrolite (Ntr) matrix. **(c)** Prismatic fluorapatite with a thin coating of Sr-rich apatite/fluorcaphite on the natural rock fracture. **(d)** Section through the fluorapatite (Fap) crystal partially edged by Sr-rich apatite or fluorcaphite (Sr–Fap/Fcp) in the natrolite matrix. **(e)** Ti-rich magnetite altered to uncertain titanomaghemite accompanied by the annitic mica. **(f)** Slawsonite (Sws) and annitic mica (Ann) pseudomorph after unidentified mineral.

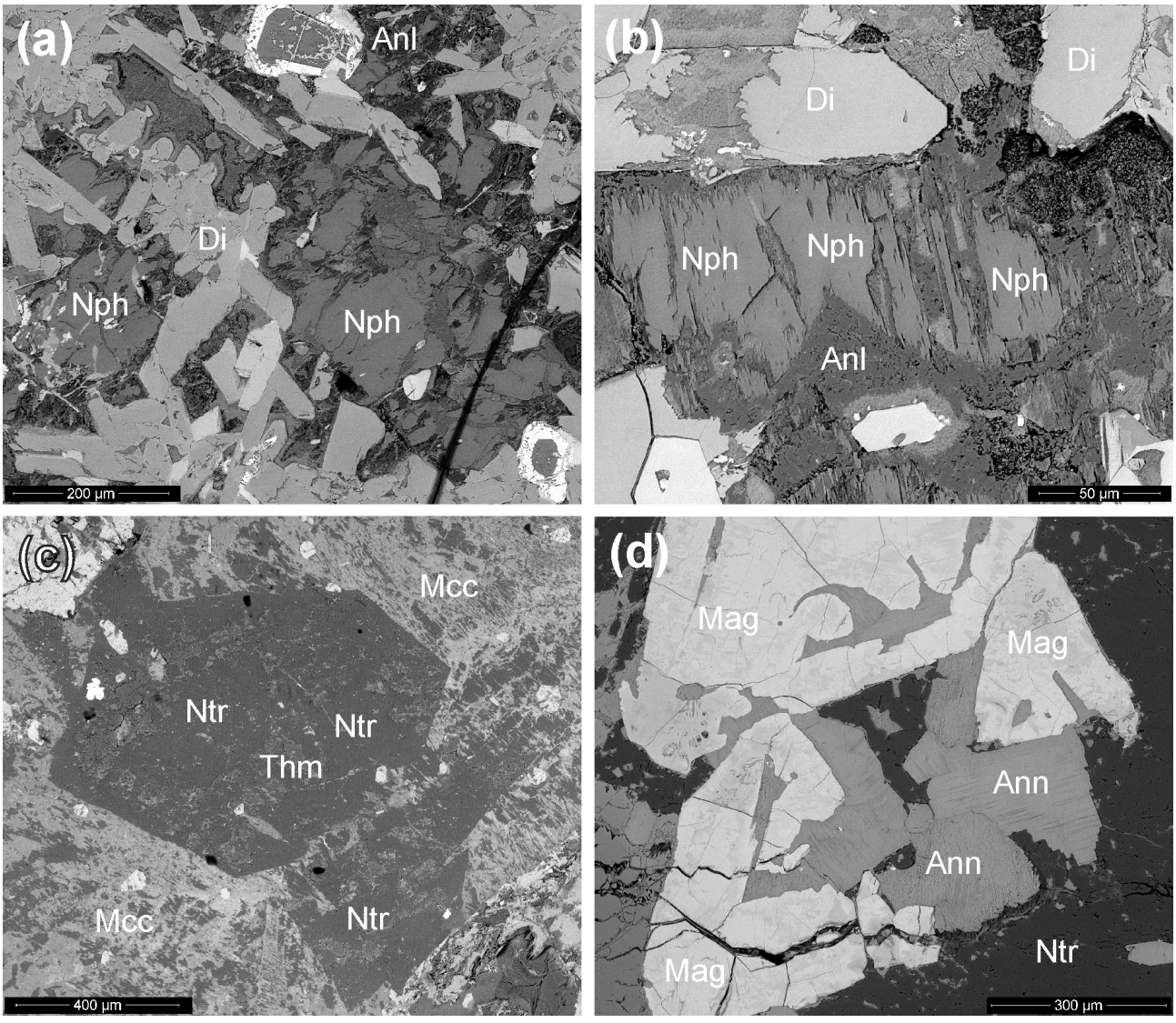

Figure 5. BSE images of the minerals from Brušperk–Borošín site no. 3 **(a, b)** and Bruzovice–Pazderůvka **(c, d)**: **(a)** fractured subhedral nepheline (Nph) partially altered to analcime (Anl) surrounded by euhedral diopside (Di) crystals, **(b)** nepheline (Nph) more progressively altered to analcime (Anl), **(c)** pseudomorphs after feldspathoid (nepheline or sodalite) composed of prevailing natrolite (Ntr) over patchy thomsonite (Thm) in the matrix dominated by microcline (Mcc), and **(d)** altered skeletal Ti-rich magnetite (Mag) with annite (Ann) surrounded by the natrolite (Ntr) matrix.

(Fig. 5a) between pyroxene crystals and is strongly replaced from the edges by analcime (Fig. 5b). The WDS microanalyses of nepheline are shown in Table S3. The Si/Al ratio of nepheline from Borošín 3 ranges from 1.05 to 1.11, and the Na/K ratio ranges from 3.43 to 3.93. The variability in the nepheline composition is generally quite large, and the analyses presented here are not out of line with those in the literature (e.g. Wilkinson and Hensel, 1994; Henderson, 2020). The unit-cell parameters of the nepheline are fully comparable with those in published data (see Table S2).

5.1.3 Bruzovice–Pazderůvka locality

The Bruzovice–Pazderůvka locality is comprised of a natural outcrop of medium-grained mafic volcanites situated in a notch of the creek. Leucocratic, non-contrastingly bordered coarse-grained rocks partly rich in amphiboles have been observed locally.

The results of PXRD analyses and SEM/EDS indicate that these are variably amphibolic and also amphibolic–pyroxenitic rocks with a fully altered zeolitic matrix consisting of natrolite, analcime, and microcline. The groundmass is heterogeneous, containing areas dominated by relatively homogeneous analcime and areas of with a predominance

of natrolite. The potassium feldspar is lath-like and euhedral to the natrolite. Overgrown fibrous clusters and maps of Na–Ca zeolites, probably thomsonite occur, locally in the natrolitic mass. Natrolite-rich areas occasionally show (pseudo-)hexagonal habits (Fig. 5c), which may represent pseudo-morphoses after the feldspathoids. Fe–Ti oxides (Ti-rich magnetite) are altered and frequently intergrown with Fe-bearing micas – annite (Fig. 5d).

5.2 Selected accessory minerals

5.2.1 Perovskite subgroup minerals and Ca–LREE–titanoniobate

Loparite and lueshite have been recognised at Brušperk–Borošín site no. 1, and only loparite was found in Bruzovice–Pazderůvka. The minerals usually take the form of polygonal or anhedral grains or, more rarely, show signs of cubic habits (Fig. 6a, b). Their size is usually up to 25–30 µm (max. of 40 µm).

Examples of the composition of this type with the recalculation of structural formulae and percentage shares for the end-member composition are given in Table S5. Projections of microchemical analyses are presented in the classification diagrams. The majority of spots fall into the strontian–calcium loparite field within the tausonite–perovskite–loparite diagram (Fig. 7a), with only one analysis corresponding to calcian–strontian loparite. In the lueshite–perovskite–loparite classification diagram (Fig. 7b), most analyses correspond to niobian–calcian loparite; only two analyses fall on the edge of the ceroan–calcian lueshite field. The end-member shares, apart from those in the two above-mentioned analyses, show a slight predominance of the loparite component (mean = 36 %) over the lueshite component (mean = 32 %). Nevertheless, the tausonite (18 %) and pyrochlore (13 %) components are also significantly represented. Other components occur in average proportions below 0.5 % (Table S5). For these reasons, the mineral may be regarded as loparite with a composition very close to the middle member of the series between loparite and lueshite.

None of the WDS microanalyses provided all REEs above the detection limit. Relatively low abundances are found mainly for Gd, Tb, Ho, Lu, and occasionally Y. The mineral shows a very slight positive Ce anomaly ($Ce/Ce^* = 0.99$ to 1.4), and in the cases of analyses where Gd is above the detection limit, it also shows a significant positive Eu anomaly ($Eu/Eu^* = 1.7$ to 10.7). However, this anomaly is caused by extremely low Gd levels and occasionally lower levels of Sm. The contents of the other cations (Mg, Mn, Pb, Zn, P, As, Sn, Sc, Y, Tb, Ho, Er, Tm, Yb, Lu, and Cl) are below the detection limit.

The Ca–LREE–titanoniobate rarely accompanied loparite at Brušperk–Borošín site no. 1. Its appearance is very similar to loparite – it forms polygonal grains with a size of 20–60 µm. They are clearly altered from the outer rim. More internally, a microfibrous zone has evolved in such grains, probably formed by a mixture of silicates and oxides. The composition of the grain cores shows high proportions of Ti, Nb, Ca, and Ce but with virtually no Na (Table S6). Its average formula based on 11 spots can be written as $(Ca_{1.41}Sr_{0.01}LREE_{0.75}Fe^{3+}_{0.07}Al_{0.01}Th_{0.02})_{\Sigma=2.27}(Ti_{2.58}Nb_{1.58}Ta_{0.04}Si_{0.14}Zr_{0.01})_{\Sigma=4.34}(O_{11.95}F_{0.05})_{\Sigma=12.00}\cdot nH_2O$. The Ti/Nb ratio varies from 1.0 to 2.3, with an average of 1.6. REEs are dominated by LREE, namely Ce and La. The ThO_2 content is elevated compared to loparite (average 0.59 wt %, maximum 1.90 wt %). The K, Mg, Mn, Pb, Zn, As, Sn, W, Sc, Gd, heavy rare earth elements (HREEs), and Cl contents are below the detection limit.

5.2.2 Pyrochlore group minerals

A detailed investigation of textural patterns and mutual relationships with the accompanying minerals revealed that members of the pyrochlore group are only minor-to-rare accessories in TAR occurrences in the following order of decreasing frequency: Nový Jičín–Čerťák → Bruzovice → Brušperk–Borošín. Pyrochlore forms small, homogeneous, mostly unaltered grains ($\leq$ 30 µm, see Fig. 8) that are locally closely accompanied by zircon (Fig. 8f).

Calcium is a dominant cation at the *A* site in pyrochlores (Fig. 9a, b; Tables S7 and S8) in Nový Jičín–Čerťák ($\leq$ 1.55 apfu Ca) and Bruzovice ($\leq$ 1.46 apfu Ca), but significantly lower content is characteristic of pyrochlore from Brušperk–Borošín ($\leq$ 0.77 apfu). The contents of Na at Nový Jičín–Čerťák and Bruzovice are comparable ($\leq$ 0.62 and 0.64 apfu Na); however, at Brušperk–Borošín, pyrochlore is Na-free (Fig. 9b). The concentrations of LREE (Ce + La + Pr + Nd + Sm) are similar at Nový Jičín–Čerťák ($\leq$ 0.14 apfu) and Bruzovice ($\leq$ 0.01 apfu) but higher at Brušperk–Borošín ($\leq$ 0.23 apfu). Trace concentrations of U ($\leq$ 0.05 apfu), Th ($\leq$ 0.02 apfu), and Y ($\leq$ 0.01 apfu) are typical in most of the compositions (Tables S7 and S8). Pyrochlores from Nový Jičín–Čerťák and Bruzovice are characterised by full to decreased occupancy in the *A* site relative to compositions from Brušperk–Borošín, where more than 50 % of the *A* sites are vacant or are filled with H_2O (Fig. 9b; Tables S7 and S8).

The Ta/(Ta + Nb) ratio is very low and its range limited in all compositions of the TARs (0.01–0.04; Tables S7 and S8). The concentrations of Ti increase in pyrochlores from Nový Jičín–Čerťák ($\leq$ 0.59 apfu Ti) through Bruzovice ($\leq$ 0.69 apfu Ti) to Brušperk–Borošín ($\leq$ 0.78 apfu Ti; Fig. 9c; Tables S7 and S8). An inverse and only small trend is obvious in the Zr contents (Brušperk ca. $\leq$ 0.01 apfu → Bruzovice $\sim\leq$ 0.09 apfu → Nový Jičín–Čerťák $\sim\leq$ 0.26 apfu; Tables S7 and S8). Minor-to-trace concentrations of Ta ($\leq$ 0.05 apfu), Si ($\leq$ 0.14 apfu), Al ($\leq$ 0.07 apfu), and Fe^{3+} ($\leq$ 0.14 apfu) are characteristic at the *B* site of most compositions.

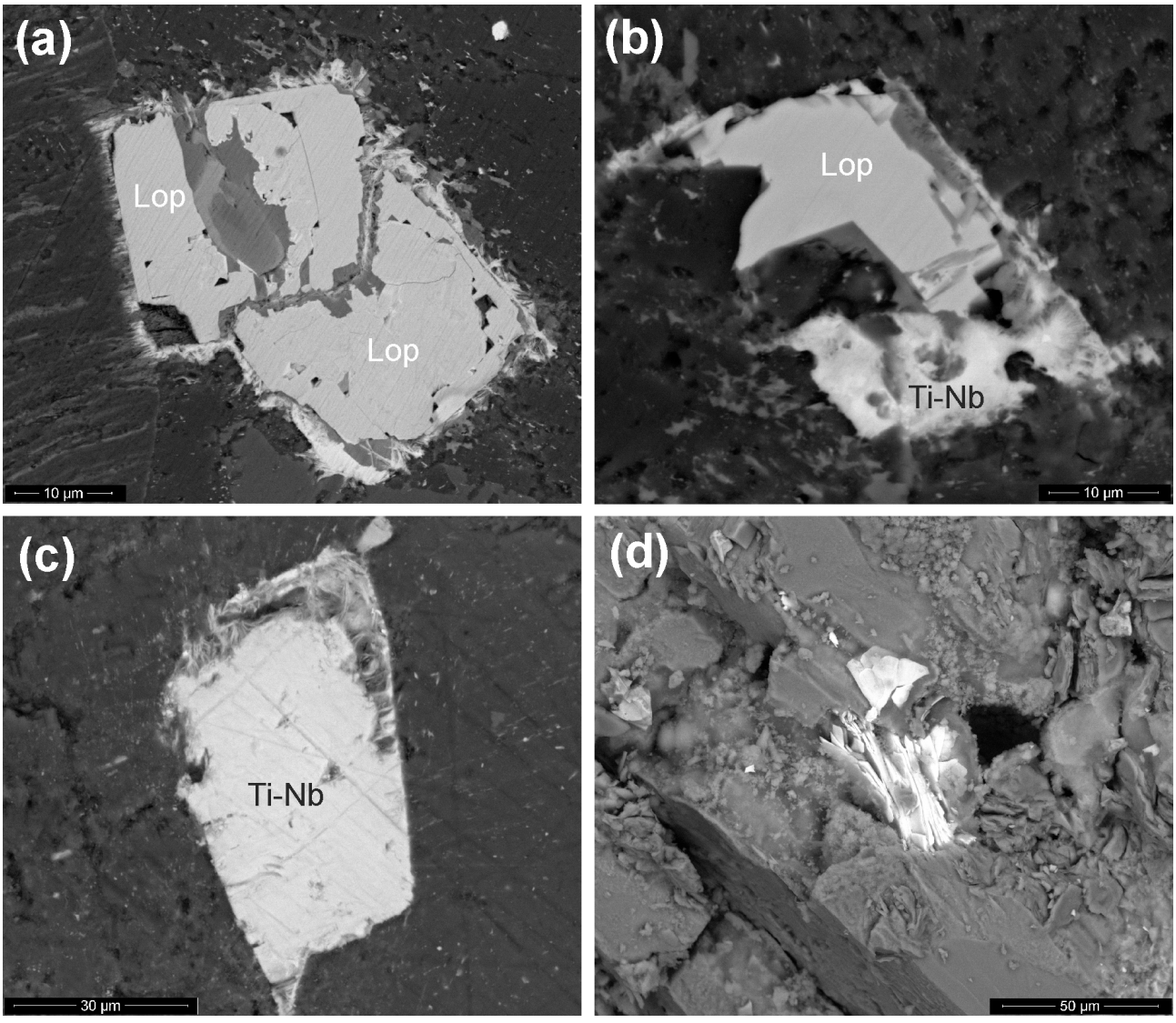

Figure 6. BSE images of the minerals from Brušperk–Borošín site no. 1: **(a)** euhedral loparite (Lop) twin, **(b)** loparite (Lop) accompanied by Ca–LREE–titanoniobate (Ti-Nb), **(c)** partially altered Ca–LREE-titanoniobate (Ti–Nb) crystal, and **(d)** REE–fluorocarbonate (white) on the natural rock fissure.

Pyrochlores from TARs are generally enriched in F (Fig. 9d); the highest-ever detected F content in TARs ($\leq$ 1.05 apfu; Tables S7 and S8) was observed in pyrochlore from Nový Jičín–Čerťák. The analytical totals are locally decreased, probably due to the "water" content. The pyrochlore compositions from Nový Jičín–Čerťák and Bruzovice correspond to a Ca-dominant member of the *A* site (Fig. 9a, b and Tables S7 and S8), with the analytical totals (93.3 wt %–99.9 wt %), total O (6.64–6.22 apfu), and finally F (0.38–1.05 apfu). Pyrochlore from the Brušperk–Borošín locality is impoverished in Ca ($\leq$ 0.77 apfu) and the other *A*-site constituents; therefore, the zero-valence-dominant member of the *A* site prevails (Fig. 9a, b and Tables S7 and S8). Optimal or slightly elevated analytical totals (99.7 wt %–101.1 wt %), lower total O (5.21–5.28 apfu), and similar F content (0.65–0.81 apfu) were observed compared to the compositions mentioned above.

5.2.3 Stronalsite

Stronalsite was identified in seven samples of leucocratic dikes coming from the Nový Jičín–Čerťák locality. It forms microscopic anhedral and distinctively foliated aggregates, accompanied by more frequent slawsonite (Fig. 11). Stronalsite reaches up to 1 mm, but it is not distinguishable with the naked eye from the surrounding matrix. The matrix is formed of a micecaous phase of illite–paragonite composition, a fine-grained mixture of natrolite and Sr-rich thomsonite-(Ca)

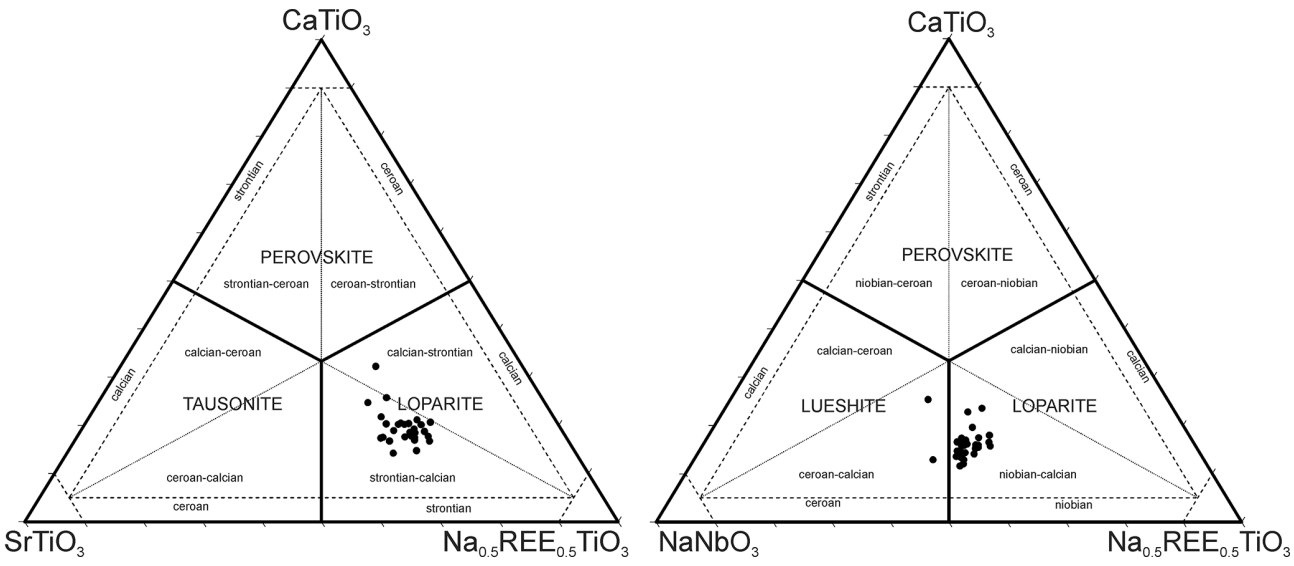

Figure 7. Composition (mol. %) of the Brušperk–Borošín microanalyses in the tausonite ($SrTiO_3$)–perovskite ($CaTiO_3$)–loparite ($Na_{0.5}REE_{0.5}TiO_3$) and lueshite ($NaNbO_3$)–perovskite ($CaTiO_3$)–loparite ($Na_{0.5}REE_{0.5}TiO_3$) diagrams.

without K–Na feldspars. Two grains of Na–Ca–Sr alumosilicate, possibly related to lisetite, were discovered, but a detailed characterisation was not performed due to their size.

Stronalsite microchemical analyses are given in Table S9. Its average formula based on 10 spots can be written as $(Na_{1.98}K_{0.3})_{\Sigma=2.01}(Sr_{0.73}Ba_{0.14}Ca_{0.01}Fe_{0.01})_{\Sigma=0.90}Al_{3.92}Si_{4.11}O_{16.00}$. It is clear that the stronalsite component is dominant (75 % to 87 %) over the banalsite component (10 % to 25 %); the share of the Ca component (lisetite) does not exceed 3.4 %, and the potassium content is very low. There is a minor but obvious discrepancy between WDS and EDS results – the average Si content is 0.112 apfu higher in the case of WDS, while Al content is on average 0.115 apfu lower. However, the average difference in sodium content is only 0.018 apfu, which is probably related to the different chemistry of measured crystals and not to the systematic error caused by the higher-energy-beam use. The barium content is higher in stronalsite compared to in slawsonite (Ba/Sr + Ba is 10 %–25 % in the case of stronalsite but 4 %–10 % in the case of slawsonite). Stronalsite internal zoning is locally apparent in BSE images; consequently, darker cores and lighter rims are caused by the variable application of the Sr/Ba distribution within individual grains.

5.2.4 Zircon, baddeleyite, REE–fluorocarbonate

Other interesting accessory minerals include zircon (Nový Jičín–Čerťák) from all types of local rocks, sometimes even as euhedral octahedrons of up to 30 µm accompanied by much rarer aggregates of tabular baddeleyite.

A platy aggregate of REE–fluorocarbonate was recognised at the Brušperk–Borošín no. 1 and Bruzovice sites (Fig. 6d). Its chemical microanalysis is listed in Table S10. However, its chemical formula was not calculated due to uncertainty about its theoretical formula and the water/hydroxyl content in its structure. From the composition itself, it seems to be related more to fluorocarbonate with an additional $(PO_4)^{3-}$ anion group, such as daqingshanite-(Ce), rather than related to minerals such as synchysite-(Ce). However, it contains more than twice the amount of Ce_2O_3 and La_2O_3 compared to daqingshanite-(Ce), with less than half the amount of SrO (Ren et al., 1983). An extremely rare phase (< 10 grains), with a high proportion of Nb, Y, and REE and with a predominance of Ce, also came from Brušperk–Borošín. This phase contains almost no Ti. The mineral has not been studied in detail due to its rarity and very limited size; the EDS spectrum suggests possibly nioboaeschynite-(Ce).

6 Discussion

Natrolitised nepheline-bearing rocks are probably not rare in nature, but detailed descriptions of them are available for only a few places worldwide, namely the most prominent alkaline and peralkaline complexes. We can mention, for example, Lovozero Massif, Kola Peninsula, Russia, where several nepheline- and sodalite-bearing rocks (lujavrite, foyaite, nepheline, and foid syenites) underwent auto-metasomatic alterations, producing natrolite and a number of rare accessory minerals (e.g. Mikhailova et al., 2023; Mokrushina et al., 2023). Natrolite and analcime are typical alteration products of nepheline transformation at Poços de Caldas potassic alkaline complex, southeast Brazil (Guarino et al., 2021), or at Ilímaussaq alkaline complex, Greenland (Rose-Hansen and Sørensen, 2002). Such massifs share some mineralogical similarities with the rocks that we studied, apart from the

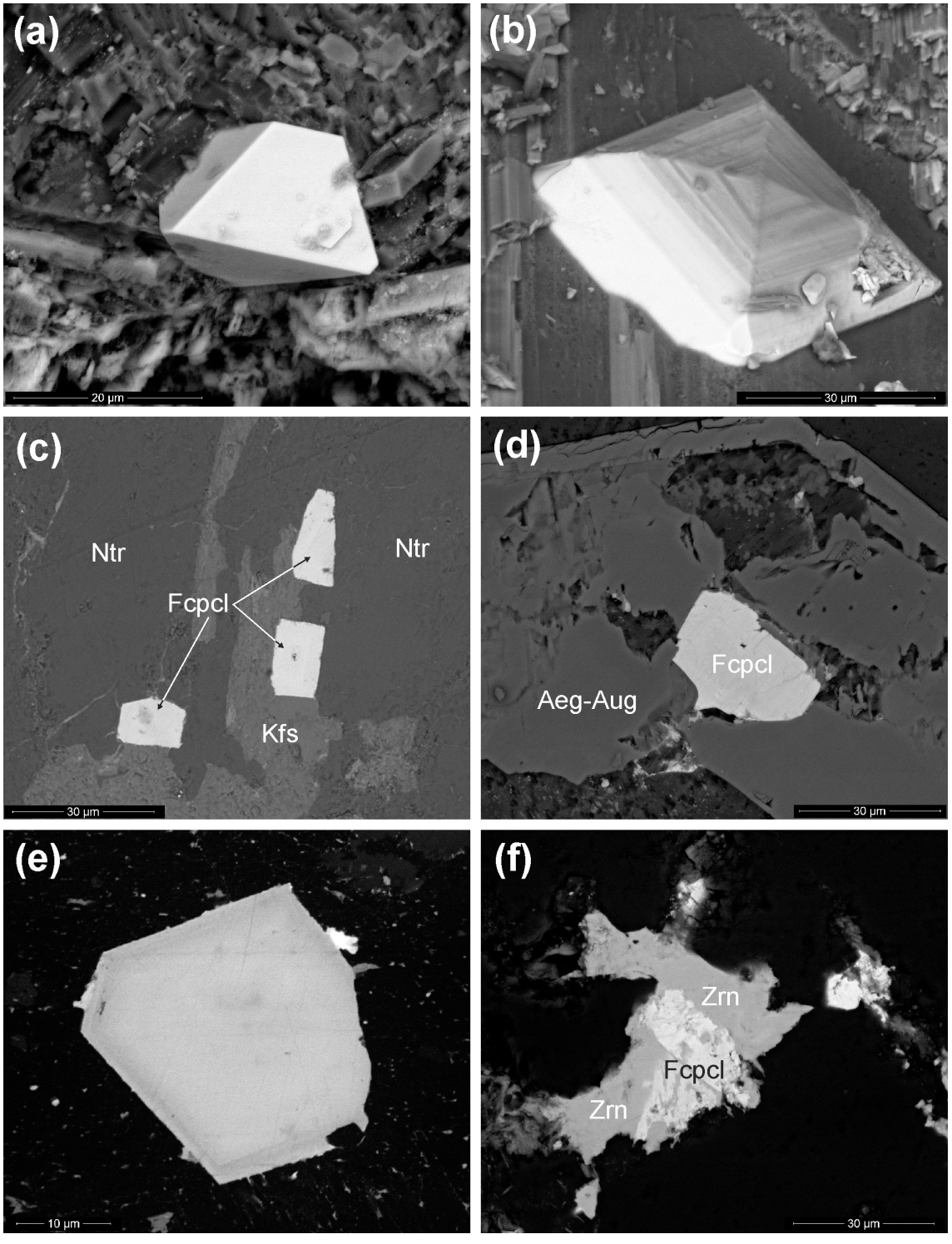

Figure 8. BSE images of the fluorcalciopyrochlores (Fcpcl): **(a)** octahedral habit, **(b)** step growth, **(c)** crystals embedded in a K–feldspar (Kfs) and natrolite (Ntr) vein, **(d)** crystal situated within the aegirine–augite (Aeg–Aug) aggregate, **(e)** euhedral slightly zoned pyrochlore, and **(f)** pyrochlore surrounded by the anhedral zircon (Zrn). **(a, b)** Natural rock fractures and **(c–f)** polished sections. Localities: **(a–c)** Nový Jičín–Čerťák **(d)**, Borošín no. 1 site, and **(e, f)** Bruzovice.

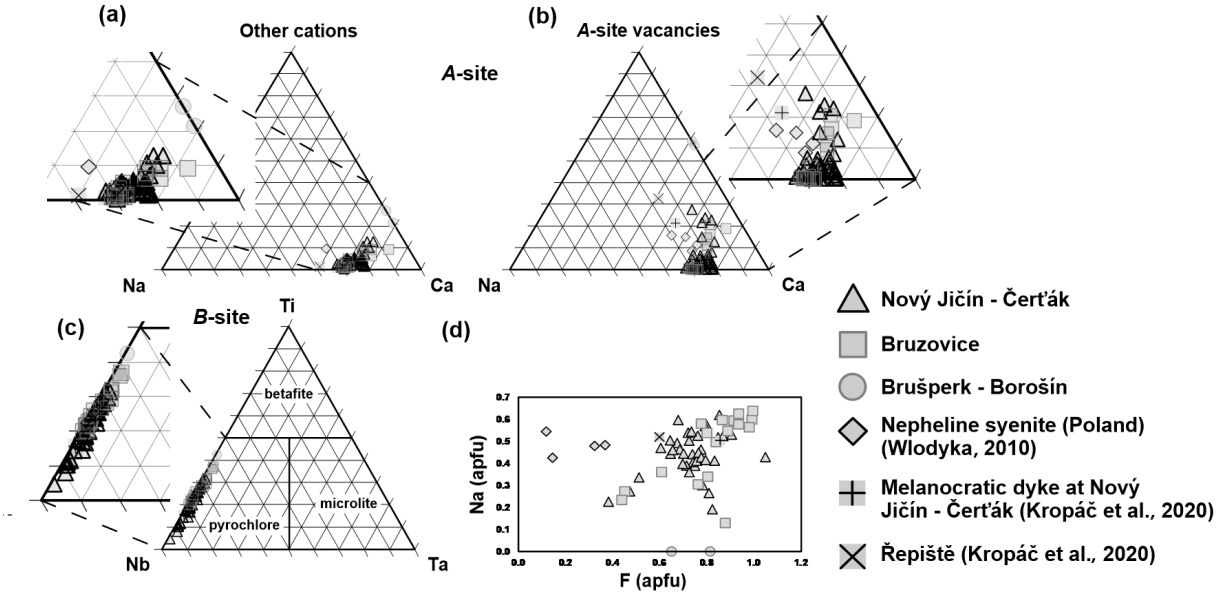

Figure 9. Ternary classification diagrams and F–Na plot for pyrochlore group minerals in TARs: **(a)** *A* site (Na–Ca–other cations), **(b)** *A* site (Na–Ca–vacancy), **(c)** *B* site (Nb–Ta–Ti), and **(d)** F vs. Na plot. Note that "other cations" represent U, Th, LREE, Y, Mn, Pb, and Zn in the *A* site.

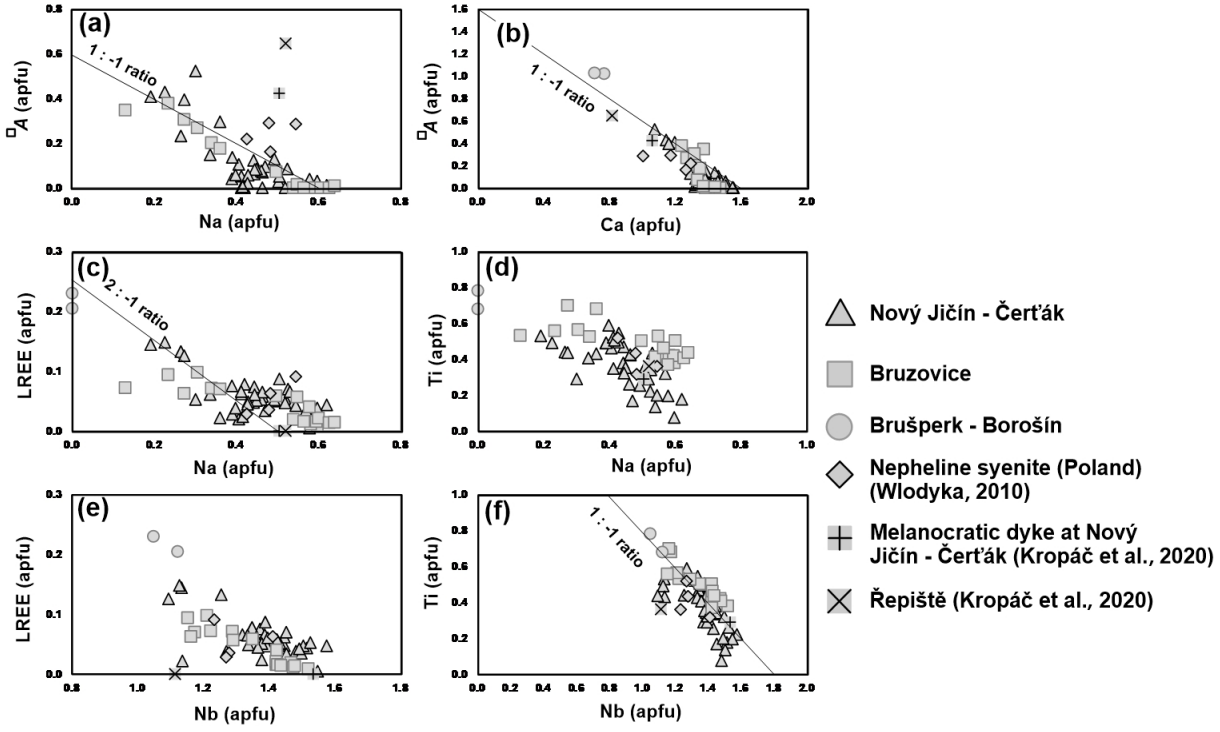

Figure 10. Correlations of elemental concentrations in atoms per formula unit (apfu) in pyrochlore group minerals in TARs: **(a)** Na vs. a vacancy in the *A* site; **(b)** Ca vs. a vacancy in the *A* site; **(c)** Na vs. LREE; **(d)** Na vs. Ti; **(e)** Nb vs. LREE; **(f)** Nb vs. Ti. Note that "LREE" represents Ce, La, Pr, Nd, and Sm.

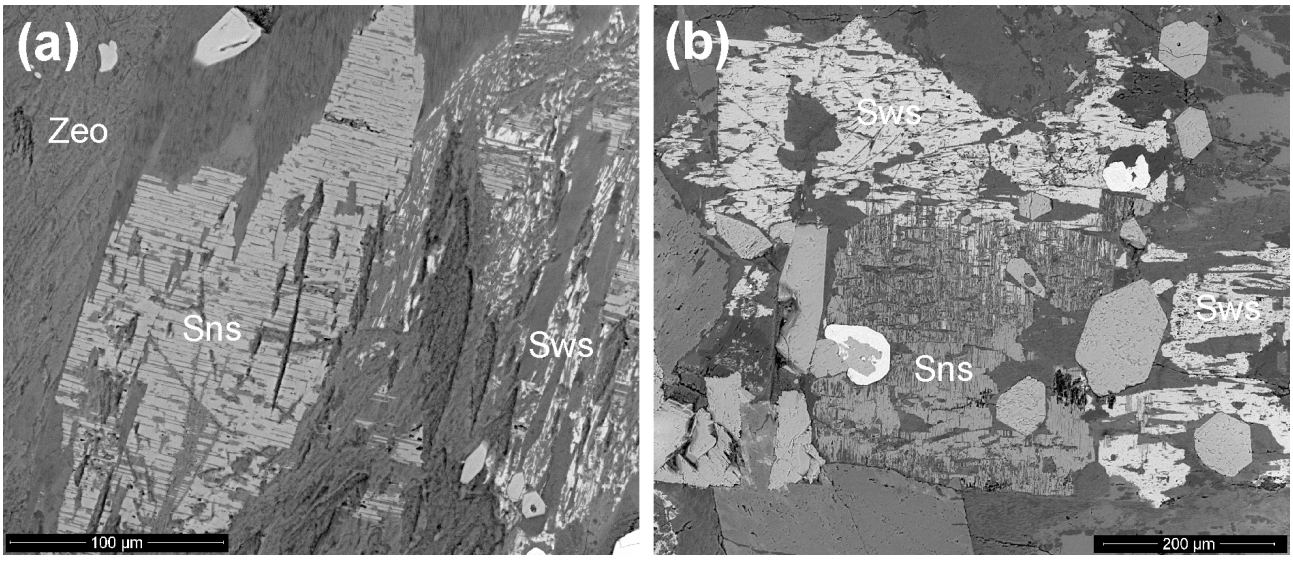

Figure 11. BSE images of the stronalsite from the Nový Jičín–Čerťák locality: **(a)** stronalsite (Sns) and slawsonite (Sws) in the zeolite (Zeo) matrix and **(b)** stronalsite (Sns) and slawsonite (Sws) with euhedral diopsides in the zeolite matrix.

natrolitised feldspathoids, such as the presence of aegirine, diopside, fluorapatite, and loparite.

Since we do not know of any unaltered nepheline-bearing TARs, it is hard to conclude which elements were mobilised in the nepheline alteration process. However, apart from the obvious activity of Na^+ and K^+, the presence of secondary Ba–feldspars (celsian) and Sr-bearing phases (slawsonite, stronalsite, Sr-rich apatite, fluorcaphite, and strontiofluorite) is evidence for the release of barium and strontium, possibly from feldspathoids, primary Na–Ca feldspars (oligoclase to bytownite), and optionally also from glass (if present).

The natrolitisation was obviously a very low-temperature process, which did not affect most of the primary minerals, including accessories. Virtually no zoning was noticed during the study of pyrochlore group minerals or loparite. This is in line with the anticipated temperature of such an alteration. The cooling of late-stage magmatic fluids represents some kind of retrograde metamorphism. From the TARs, the estimated aegirine crystallisation temperatures range between 510 and 390 °C (Dolníček et al., 2010a) in the sub-solidus state (Rapprich et al., 2024). The presence of epidote and prehnite indicates a temperature range of ∼ 200–300 °C at Nový Jičín–Čerťák, and the presence of the chlorite group mineral(s) indicates a temperature range of ∼ 225–300 °C for Borošín and Bruzovice (Chipera and Apps, 2001). We can expect temperatures of ∼ 250–150 °C for the natrolite transformation from nepheline and of ∼≤ 150 °C for the natrolite to analcime transformation, analogous to the Mont Saint-Hilaire Complex, Quebec, Canada (Schilling et al., 2011). However, natrolitised TARs are just a small portion of the TARs, while the majority is dominantly analcimised, with no evidence of the nepheline pseudomorphs. Whether the precursor for the more common analcimisation was also nepheline is unclear at this moment.

The first intriguing specific observation is the presence of rare albite relics within K–feldspar aggregates in the leucocrate parts of the mafic rocks and the matrix of the leucocratic dikes. This indicates potassium metasomatism and a phase imbalance in the rocks, as there is a reaction of natrolite + albite = analcime, and the coexistence of these phases cannot exceed ∼ 100 °C (Velde, 1985).

The composition of loparite and lueshite from the natrolitised TARs varies significantly from the other occurrences worldwide; when plotting the end-member compositions on the perovskite–lueshite–loparite diagram (Fig. 12), they are closest to the ones from the Lovozero and Khibiny complexes, Kola Peninsula, Russia, but are significantly enriched in the perovskite (calcian) component. This is probably due to the presence of Ca–Na feldspars in the pre-altered rocks.

The description of Ca–LREE–titanoniobate presents an intriguing question since no mineral with a similar composition has been described so far. It might be related to belyankinite, considering its close association with loparite and its occurrence in the peralkaline rocks. Belyankinite – possibly $Ca_{1-2}(Ti,Nb)_5O_{12}\cdot 9H_2O$ – was described for the first time in the Medvezh'ya Berloga pegmatite in the Lovozero area in Russia by Gerasimovskii and Kazakova (1950). It occurs in several peralkaline pegmatites of the Lovozero alkaline complex, Kola Peninsula, predominantly as pseudomorphs after Ti-rich silicates (Semenov, 1957; Vlasov et al., 1966). This mineral was also reported in 20–30 µm thin metasomatic alteration rims of loparite, enriched in $LREE_2O_3$ and ThO_2, from the Khibina alkaline complex, Kola Peninsula. The high thorium content is responsible for the metamict state of the phase, which is X-ray amorphous prior to heating

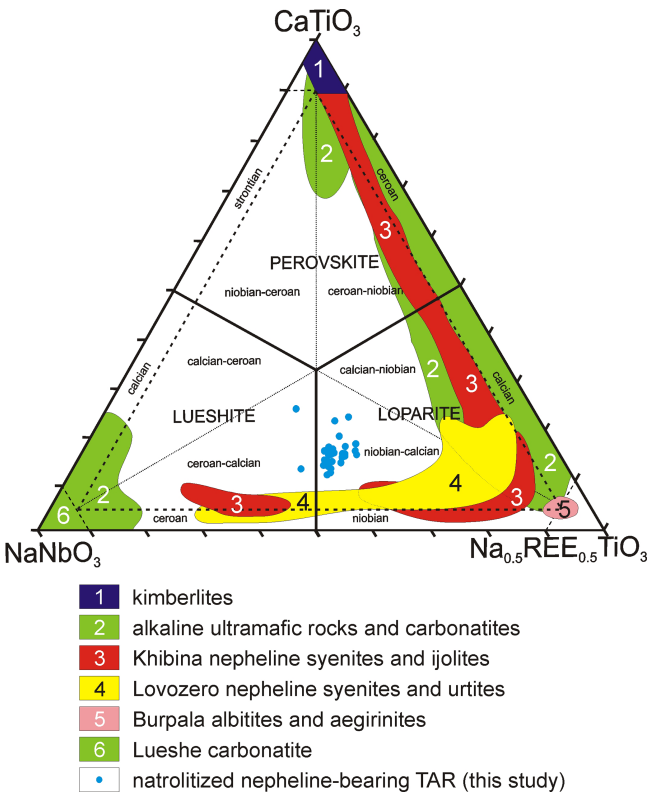

Figure 12. Compositional variation (mol. %) of perovskite-group minerals from various rock suites and localities (according to Mitchell et al., 2017) given on the perovskite–lueshite–loparite diagram and their comparison with the samples studied.

(Mitchell and Chakhmouradian, 1998). Apart from in Russia, belyankinite was described in the REE-bearing lithium–caesium–tantalum (LCT) granitic pegmatites in the Southeastern Desert of Egypt. It forms thin replacement rims rich in ThO_2 (up to 18 wt %) on the Nb-rich loparite cores (Saleh, 2007). However, some authors suggest that belyankinite is a mixture of minerals with prevailing anatase (Yakovenchuk et al., 2005).

The problem is that various authors offer various crystalo-chemical formulae for this phase: $Ca_{1-2}(Ti,Nb)_5O_{12}\cdot 9H_2O$ (Gerasimovskii and Kazakova, 1950), $Ca_{0.9}(Ti,Zr,Nb,Si)_{5.5}O_{12}\cdot 10H_2O$ (Semenov, 1957), or $(Ca_{0.71}Na_{0.07}Mg_{0.06}Mn_{0.06}LREE_{0.70}Th_{0.96})_{\Sigma=2.54}(Ti_{4.13}Si_{2.29}Nb_{1.61}Fe^{3+}_{0.98})_{\Sigma=10.03}O_{24.00}\cdot nH_2O$ (Mitchell and Chakhmouradian, 1998), none of which corresponds to the composition we obtained from the Ca–LREE–titanoniobate in this study (Ca + LREE / Nb + Ti $\sim$ 0.5). Other available options based on the microchemical composition are, for example, still undescribed Nb-analogues of cafetite or kassite. However, it is not possible to completely rule out the option that the phase investigated is in fact of a nanocrystalline mixture, although the SEM images do not correspond to this.

From the minerals investigated, only the pyrochlore group minerals were described previously in the study area. Four microchemical analyses of the nepheline syenite veins from Puńców, Poland, were published by Włodyka (2010). The author avoided their classification, but according to our study (Figs. 9 and 10), they all fall within the field of hydroxycalciopyrochlore. The second and last observations of pyrochlore group minerals came from Kropáč et al. (2020), who described them at both Čerťák near Nový Jičín (the site investigated in this article; Figs. 9 and 10) and Řepiště (leucocratic nest in analcime "teschenite"). For both analyses published, it is not clear if they are average ones or single spots (the authors state "representative compositions"); both are missing some important elements (e.g. strontium), have an analytical sum < 90 %, and fit within fluorcalciopyrochlore. Kropáč et al. (2020) considered such a primary magmatic phase at the localities. The pyrochlores that we investigated from the two sites are *A*-site Ca-dominant members with F ranging from 0.38 to 1.05 apfu, which could be classified as fluorcalciopyrochlore, hydroxycalciopyrochlore, or oxycalciopyrochlore. The last locality yielded an *A*-site zero-valence-dominant member with F content 0.65–0.81 apfu, indicating the presence of the IMA-unapproved possible member fluorkenopyrochlore (Atencio et al., 2010). Nevertheless, at the latter locality, we have a lack of compositional data on pyrochlore crystal chemistry; therefore, the presence of these possible members is only speculative.

Compositional trends in individual pyrochlores in TAR occurrences were examined in detail, and the following correlations between *A* and *B* constituents and *A*-site vacancy are demonstrated in Fig. 10. A positive correlation between F and Na (Fig. 9d) and a negative relation between Na and *A*-site vacancy (Fig. 10a) suggest a dominant substitution:

$$^{A}Na^{Y}F^{A}\square^{Y}_{-1}\square_{-1}. \quad (1)$$

A negative correlation between Ca and *A*-site vacancy (Fig. 10b) suggests the following substitution (2):

$$^{A}Ca^{Y}O^{A}\square^{Y}_{-1}\square_{-1}. \quad (2)$$

The correlation vector between Na and LREE close to ~ -2 (Fig. 10c), a negative correlation between Na and Ti (Fig. 10d) and between Nb and LREE (Fig. 10e), and finally the correlation vector between Nb and Ti at ~ -1 (Fig. 10f) can be expressed via the following substitution (3):

$$^{A}Na_2{}^{B}Nb^{A}LREE^{B}_{-1}Ti_{-1}. \quad (3)$$

The presence of stronalsite is closely related to the slawsonite and K– and Ba–feldspars, as anticipated by Hori et al. (1987). Minor isomorphic admixtures of Ca and K were noticed in its other global occurrences (e.g. Liferovich et al., 2006b; Zozulya et al., 2009), while the substitution $Sr^{2+} \leftrightarrow Ba^{2+}$ is typical of the stronalsite–banalsite solid-solution series (Liferovich et al., 2006a). In agreement with Liferovich et

al. (2006a, b), we must conclude that the local formation of stronalsite and slawsonite is related to the late-stage magmatic processes, where these minerals are formed in a subsolidus reaction of primary nepheline (and possibly also Na–Ca feldspar) with a deuteric alkaline fluid. Strontium activity of during the late-stage magmatic processes is also reflected by the presence of Sr-rich rims on fluorapatite. A similar phenomenon was noticed, for example, by Guarino et al. (2021) from the Poços de Caldas alkaline complex, Brazil.

7 Conclusions

The Teschenite Association rocks represent a rather unique example of nepheline (and possibly other feldspathoid mineral) late-stage alteration in the case of small batches of magma and open systems allowing fluid migration and ion exchange with the surrounding sediment pore water and/or seawater. There are many similarities to the large alkaline and peralkaline massifs of the world, but due to the smaller size of the igneous bodies (sills ca. dozens rather than hundreds of metres in size), we must expect only limited amounts of sodium and potassium released into the late-stage hydrothermal fluids by the feldspathoid alteration. Additionally, the pre-altered rocks were probably closer to melanocratic nephelinolites (melteigites) than to ijolites in some cases, which also affected the mass balance of the alteration processes.

The transformations observed affected primary mineral assemblage by mobilisation of $Na^+ > K^+ > Ba^{2+}$, Sr^{2+}, and Ca^{2+} ions during the sub-solidus (late hydrothermal) stage of the magma cooling, generally below 300 °C. There are no completely unaltered nepheline-bearing TARs to compare with, but evidence from the primary mineral relics (Na–Ca feldspars, feldspathoids) indicates that their decomposition was main driving force of composition changes of the late hydrothermal fluids. The presence of a glass component in the phaneritic rocks is not probable but cannot be completely neglected.

Due to the very low-temperature character of rock matrix natrolitisation, some of the primary minerals, including accessories, were not affected. However, the phases studied, including pyrochlore group minerals and Sr-rich phases (stronalsite and slawsonite), show important processes related to the hydrothermal (auto-)metasomatic stage of the rock development. In the case of the perovskite group minerals, alteration is present only rarely, showing as the uncertain Ca–LREE–titanoniobate phase.

The rather unique chemical composition of loparite and lueshite (see Mitchell et al., 2017) belonging to the hydrothermal stage reflects enrichment in the perovskite (calcian) component, which could be explained by the presence of Ca–Na feldspars in the pre-altered rocks. Higher activity of Ca^{2+} ions is also documented by the presence of newly formed thomsonite–Ca and prehnite. Some of the loparites are partially or completely transformed into Ca–LREE-rich niobium titanosilicate, which represents the youngest alteration process. Its chemical composition does not correspond to any known mineral phase. Its thorium content is rather low (average 0.02 apfu), so its origin must be connected to hydrothermal alteration rather than to metamict transformation like the somewhat-comparable mineral belyankinite, which has a questionable status (Mitchell and Chakhmouradian, 1998).

Prior to this study, there were only six available analyses of the pyrochlore group minerals from TARs, falling into the hydroxycalciopyrochlore and fluorcalciopyrochlore fields. Our investigation proved its presence at all natrolitised TAR sites investigated. Two of them are Ca-dominant members at the *A* site with F contents between 0.38 and 1.05 apfu, which could be classified as fluorcalciopyrochlore, hydroxycalciopyrochlore, or oxycalciopyrochlore. The last site yielded grains of the zero-valence-dominant member of the *A* site with F contents 0.65–0.81 apfu, indicating the presence of the IMA-unapproved possible member fluorkenopyrochlore (Atencio et al., 2010).

The stronalsite and slawsonite, together with Sr-rich feldspars, Sr-rich zeolites, and Sr-rich members of the apatite group, represent sinks for the strontium released from the primary plagioclase and feldspathoid decomposition. They are very rare in TARs and are bound to most leucocrate rocks, suggesting a strong bond to the primary rock composition and neglecting the significant effects of fluid migration from other sources.

Data availability. All raw data can be provided by the corresponding author upon request.

Supplement. The supplement related to this article is available online at https://doi.org/10.5194/ejm-37-555-2025-supplement.

Author contributions. DM: conceptualisation, methodology, investigation, resources, data curation, writing – original draft, writing – review and editing, and visualisation. JJ: conceptualisation, methodology, investigation, resources, data curation, writing – original draft, writing – review and editing, visualisation, supervision, project administration, and funding acquisition. ŠC: investigation, writing – original draft, and visualisation. OP: investigation and writing – original draft.

Competing interests. The contact author has declared that none of the authors has any competing interests.

Disclaimer. Publisher's note: Copernicus Publications remains neutral with regard to jurisdictional claims made in the text, published maps, institutional affiliations, or any other geographical rep-

resentation in this paper. While Copernicus Publications makes every effort to include appropriate place names, the final responsibility lies with the authors.

Acknowledgements. We thank the editors and the anonymous reviewers for their constructive and helpful comments.

Financial support. The work was supported by the Czech Science Foundation (grant no. 21-30043S) and by Palacký University (grant no. IGA_PrF_2025_030).

Review statement. This paper was edited by Elena Belluso and reviewed by three anonymous referees.

References

Ahijado, A., Casillas, R., Nagy, G., and Fernández C.: Sr-rich minerals in a carbonatite skarn, Fuerteventura, Canary Islands (Spain), Miner. Petrol., 84, 107–127, https://doi.org/10.1007/s00710-005-0074-8, 2005.

Amores-Casals, S., Gonçalves, A. O., Malgarejo, J.-C., and Molist, J. M.: Nb and REE distribution in the Monte Verde carbonatite-alkaline-agpaitic complex (Angola), Minerals, 10, 10010005, https://doi.org/10.3390/min10010005, 2020.

Atencio, D.: Pyrochlore-supergroup minerals nomenclature: an update, Front. Chem., 9, 713368, https://doi.org/10.3389/fchem.2021.713368, 2021.

Atencio, D., Andrade, M. B., Christy, A. G., Gieré, R., and Kartashov, P. M.: The pyrochlore supergroup of minerals: nomenclature, Can. Mineral., 48, 673–698, https://doi.org/10.3749/canmin.48.3.673, 2010.

Bhattacharjee, S., Dey, M., Chakrabarty, A., Mitchell, R. H., and Ren, M.: Zero-valent-dominant pyrochlores: endmember formula calculation and petrogenetic significance, Can. Mineral., 60, 469–484, https://doi.org/10.3749/canmin.2100058, 2022.

Bosi, F., Hatert, F., Pasero, M., and Mills, S. J.: IMA Commission on New Minerals, Nomenclature and Classification (CNMNC) – Newsletter 80, Eur. J. Mineral., 36, 599–604, https://doi.org/10.5194/ejm-36-599-2024, 2024.

Chakhmouradian, A. R., Halden, N. M., Mitchell, R. H., and Horváth, L.: Rb-Cs-rich rasvumite and sector-zoned "loparite-(Ce)" from Mont Saint-Hilaire (Québec, Canada) and their petrologic significance, Eur. J. Mineral., 19, 533–546, https://doi.org/10.1127/0935-1221/2007/0019-1739, 2007.

Chipera, S. J. and Apps, J. A.: Geochemical stability of natural zeolites, Rev. Mineral. Geochem., 45, 117–161, https://doi.org/10.2138/rmg.2001.45.3, 2001.

Christy, A. G. and Atencio, D.: Clarification of status of species in the pyrochlore supergroup, Mineral. Mag., 77, 13–20, https://doi.org/10.1180/minmag.2013.077.1.02, 2013.

Dahlgren, S. and Larsen, A. D.: Minerals of the banalsite-stronalsite series in amygdules from the Brunlanes ultramafic volcanic series, Norsk Bergverksmuseum Skrift, 49, 93–100, 2012.

Dolníček, Z., Kropáč, K., Uher, P., and Polách, M.: Mineralogical and geochemical evidence for multi-stage origin of mineral veins hosted by teschenites at Tichá, Outer Western Carpathians, Czech Republic, Chem. Erde-Geochem., 70, 267–282, https://doi.org/10.1016/j.chemer.2010.03.003, 2010a.

Dolníček, Z., Urubek, T., and Kropáč, K.: Post-magmatic hydrothermal mineralization associated with Cretaceous picrite (Outer Western Carpathians, Czech Republic): interaction between host rock and externally derived fluid, Geol. Carpath., 61, 327–339, https://doi.org/10.2478/v10096-010-0019-y, 2010b.

Dostal, J. and Owen, J. V.: Cretaceous alkaline lamprophyres from northeastern Czech Republic: geochemistry and petrogenesis, Geol. Rundsch., 87, 67–77, https://doi.org/10.1007/s005310050190, 1998.

Dubina, O. V., Kryvdik, S. G., and Vishnevskij, O. A.: Rare earth minerals in veined nepheline syenites of the Chernihivka carbonatite massif of the Azov region, Mineral. J.-Ukraine, 44, 71–79, https://doi.org/10.15407/mineraljourna1.44.01.071, 2022.

Ferraris, C., Parodi, G. C., Pont, S., Rondeau, B., and Lorand, J.-P.: Trinepheline and fabriesite: two new mineral species from the jadeite deposit of Tawmaw (Myanmar), Eur. J. Mineral., 26, 257–265, https://doi.org/10.1127/0935-1221/2014/0026-2348, 2014.

Gerasimovskii, V. I. and Kazakova, M. E.: Belyankinite – a new mineral, Dokl. Akad. Nauk SSSR, 71, 925–927, 1950 (in Russian).

Guarino, V., Lustrino, M., Zanetti, A., Tassinari, C. C. G., Ruberti, E., de' Gennaro, R., and Melluso, L.: Mineralogy and geochemistry of a giant agpaitic magma reservoir: The Late Cretaceous Poços de Caldas potassic alkaline complex (SE Brazil), Lithos, 398–399, 106330, https://doi.org/10.1016/j.lithos.2021.106330, 2021.

Haggerty, S. and Mariano, A. N.: Strontian-loparite and strontiochevkinite: Two new minerals in rheomorphic fenites from the Paraná Basin carbonatites, South America, Contrib. Mineral. Petr., 84, 365–381, https://doi.org/10.1007/BF01160288, 1983.

Henderson, C. M. B.: Nepheline solid solution compositions: stoichiometry revisited, reviewed, clarified and rationalised, Mineral. Mag., 84, 813–838, https://doi.org/10.1180/mgm.2020.78, 2020.

Hori, H., Nakai, I., Nagashima, K., Matsubara, S., and Kato, A.: Stronalsite, $SrNa_2Al_4Si_4O_{16}$, a new mineral from Renai, Kochi City, Japan, Mineral. J., 13, 368–375, https://doi.org/10.2465/minerj.13.368, 1987.

Klvaňa, J.: Tešenity a pikrity na severovýchodní Moravě: monografie petrologická, Rozpravy Čes. akademie věd, Třída 2, 6, 1–93, 1897.

Kogarko, L. N., Williams, C. T., and Woolley, A. R.: Chemical evolution and petrogenetic implications of loparite in the layered, agpaitic Lovozero complex, Kola Peninsula, Russia, Miner. Petrol., 74, 1–24, https://doi.org/10.1007/s710-002-8213-2, 2002.

Koneva, M. A.: Banalsite and stronalsite from pyroxenites of the Zhidoy massif (the first Russian occurrence), Zapiski Vsesojuznogo Mineralogitcheskogo Obschestva, 152, 103–108, 1996.

Konopleva, N. G., Ivanyuk, G. Y., Pakhomovsky, Y. A., Yakovenchuk, V. N., and Mikhailova, Y. A.: Loparite-(Ce) from the Khibiny Alkaline Pluton, Kola Peninsula, Russia, Geol. Ore Deposit., 59, 729–737, https://doi.org/10.1134/S1075701517080049, 2017.

Kropáč, K., Dolníček, Z., Uher, P., and Urubek, T.: Fluorcaphite from hydrothermally altered teschenite at Tichá, Outer Western Carpathians, Czech Republic: composi-

tional variations and origin, Mineral. Mag., 81, 1485–1501, https://doi.org/10.1180/minmag.2017.081.016, 2017.

Kropáč, K., Dolníček, Z., Uher, P., Buriánek, D., Safai, A., and Urubek, T.: Zirconian-niobian titanite and associated Zr-, Nb-, REE-rich assessory minerals: Products of hydrothermal overprint of leucocratic teschenites (Silesian Unit, Outer Western Carpathians, Czech Republic), Geol. Carpath., 71, 343–360, https://doi.org/10.31577/GeolCarp.71.4.4, 2020.

Kropáč, K., Dolníček, Z., Uher, P., Buriánek, D., and Urubek, T.: Crystal chemistry and origin of epidote-(Sr) in alkaline rocks of the teschenite association (Silesian Unit, Outer Western Carpathians, Czech Republic), Miner. Petrol., 118, 55–70, https://doi.org/10.1007/s00710-023-00847-w, 2024.

Kropáč, K., Dolníček, Z., and Ulmanová, J.: Paragenesis, composition and origin of Ba- and Ca-rich stronalsite, a rare strontium tectosilicate, in the rocks of the teschenite association, Silesian Unit, Western Carpathians, Czech Republic, Mineral. Mag., *accepted*, https://doi.org/10.1180/mgm.2024.97, 2025.

Liferovich, R. P., Locock, A. J., Mitchell, R. H., and Shpachenko, A. K.: The crystal structure of stronalsite and a redetermination of the structure of banalsite, Can. Mineral., 44, 533–546, https://doi.org/10.2113/gscanmin.44.2.533, 2006a.

Liferovich, R. P., Mitchell, R. H., Zozulya, D. R., and Shpachenko, A. K.: Paragenesis and composition of banalsite, stronalsite, and their solid solution in nepheline syenite and ultramafic alkaline rocks, Can. Mineral., 44, 929–942, https://doi.org/10.2113/gscanmin.44.4.929, 2006b.

Locock, A. J. and Mitchell, R. H.: Perovskite classification: An Excel spreadsheet to determine and depict end-member proportions for the perovskite- and vapnikite-subgroups of the perovskite supergroup, Comput. Geosci., 113, 106–114, https://doi.org/10.1016/j.cageo.2018.01.012, 2018.

Lucińska-Anczkiewicz, A., Villa, I.M., Anczkiewicz, R., and Slaczka, A.: $^{40}Ar/^{39}Ar$ dating of alkaline lamprophyres from the Polish Western Carpathians, Geol. Carpath., 53, 45–52, 2002.

Matýsek, D. and Jirásek, J.: Occurrences of slawsonite in rocks of the Teschenite Association in the Podbeskydí Piedmont area (Czech Republic) and their petrological significance, Can. Mineral., 54, 1129–1146, https://doi.org/10.3749/canmin.1500101, 2016.

Matýsek, D. and Jirásek, J.: Corrensite and associated smectites in the Teschenite Association Rocks from the Podbeskydí Area (Czech Republic and Poland), Appl. Clay Sci., 243, 107067, https://doi.org/10.1016/j.clay.2023.107067, 2023.

Matýsek, D., Jirásek, J., Skupien, P., and Thomson, S. N.: The Žermanice sill: new insights into the mineralogy, petrology, age, and origin of the teschenite association rocks in the Western Carpathians, Czech Republic, Int. J. Earth Sci., 107, 2553–2574, https://doi.org/10.1007/s00531-018-1614-x, 2018.

Medvedeva, E. V., Nemov, A. B., and Kotlyarov, V. A.: First find of banalsite-stronalsite in Ural, Vestnik of Institute of Geology of Komi Science Center of Ural Branch RAS, 3, 13–17, https://doi.org/10.19110/2221-1381-2016-3-13-17, 2016.

Menčík, E., Adamová, M., Dvořák, J., Dudek, A., Jetel, J., Jurková, A., Hanzlíková, E., Houša, V., Peslová, H., Rybářová, L., Šmíd, B., Šebesta, J., Tyráček, J., and Vašíček, Z.: Geology of the Moravskoslezské Beskydy Mts. and the Podbeskydská pahorkatina Upland. Academia, Praha, 307 pp., 1983.

Mikhailova, J. A., Pakhomovsky, Y. A., Lyalina, L. M., and Selivanova, E. A.: Alteration of feldspathoids changes pH of late-magmatic fluids: A case study from the Lovozero Peralkaline Massif, Russia, Minerals, 13, 39, https://doi.org/10.3390/min13010039, 2023.

Mitchell, R. H. and Chakhmouradian, A. R.: Compositional variation of loparite from the Lovozero alkaline complex, Russia, Can. Mineral., 34, 977–990, 1996.

Mitchell, R. H. and Chakhmouradian, A. R.: Th-rich loparite from the Khibina alkaline complex, Kola Penninsula: isomorphism and paragenesis, Mineral. Mag., 52, 341–353, https://doi.org/10.1180/002646198547738, 1998.

Mitchell, R. H. and Chakhmouradian, A. R.: Sr-bearing perovskite and loparite from lamproite and agpaitic nepheline syenite pegmatites, Can. Mineral., 37, 99–112, 1999.

Mitchell, R. H. and Liferovich, R. P.: Subsolidus deuteric/hydrothermal alteration of eudialyte in lujavrite from the Pilansberg alkaline complex, South Africa, Lithos, 91, 352–372. https://doi.org/10.1016/j.lithos.2006.03.025, 2006.

Mitchell, R. H., Burns, P. C., and Chakhmouradian, A. R.: The crystal structures of loparite-(Ce), Can. Mineral., 38, 145–152, https://doi.org/10.2113/gscanmin.38.1.145, 2000.

Mitchell, R. H., Welch, M. D., and Chakhmouradian, A. R.: Nomenclature of the perovskite supergroup: A hyerarchical system of classification based on crystal structure and composition, Mineral. Mag., 81, 411–461, https://doi.org/10.1180/minmag.2016.080.156, 2017.

Mokrushina, O. D., Mikhailova, J. A., and Pakhomovsky, Y. A.: Fenitization at the Lovozero Alkaline Massif, NW Russia: composition and evolution of fluids, Geosci., 13, 305, https://doi.org/10.3390/geosciences13100305, 2023.

Morgenstern, R., Turnbull, R. E., Ashwell, P. A., Horton, T. W., and Oze, C.: Petrological and geochemical characteristics of REE mineralization in the A-type French Creek Granite, New Zealand, Miner. Deposita, 54, 935–958, https://doi.org/10.1007/s00126-018-0854-9, 2019.

Nickel, E. H. and Mandarino, J. A.: Procedures involving the IMA Commission on New Minerals and Mineral Names and guidelines on mineral nomenclature, Am. Mineral., 72, 1031–1042, 1987.

Pacák, O.: Sopečné horniny na severním úpatí Bezkyd moravských, Česká akademie věd a umění, Praha, 232 pp., 1926.

Petrovsky, M. N., Savchenko, E. A., and Kalachev, V. Y.: Formation of eudyalite-bearing phonolite from Kontozero carbonatite paleovolcano, Kola Peninsula, Geol. Ore Deposit., 54, 540–556, https://doi.org/10.1134/S1075701512070057, 2012.

Picha, F. J., Stráník, Z., and Krejčí, O.: Geology and hydrocarbon resources of the Outer Western Carpathians and their foreland, Czech Republic, in: The Carpathians and their foreland: geology and hydrocarbon resources, edited by: Golonka, J., Picha, J., AAPG Memoir 84, Tulsa, 49–175, https://doi.org/10.1306/985607M843067, 2006.

Platt, R. G.: Perovskite, loparite and Ba-Fe hollandite from the Schryburt Lake carbonatite complex, northwestern Ontario, Canada, Mineral. Mag., 58, 49–57, https://doi.org/10.1180/minmag.1994.058.390.05, 1994.

Popova, E. A., Lushnikov, S. G., Yakovenchuk, V. N., and Krivovichev, S. V.: The crystal structures of loparite-

(Ce): a new acentric variety, Miner. Petrol., 111, 827–832. https://doi.org/10.1007/s00710-017-0498-y, 2017.

Rapprich, V., Matýsek, D., Pour, O., Jirásek, J., Míková, J., and Magna, T.: Interaction of seawater with (ultra)mafic alkaline rocks – Alternative process for the formation of aegirine, Am. Mineral., 109, 488–501, https://doi.org/10.2138/am-2023-8928, 2024.

Ren, Y., Ximen, L., and Peng, Z.: Daqingshanite – A new mineral recently discovered in China, Geochem., 2, 180–184, https://doi.org/10.1007/BF03180107, 1983.

Rose-Hansen, J. and Sørensen, H.: Geology of the lujavrites from the Ilímaussaq alkaline complex, South Greenland, with information from seven bore holes, Danish Polar Center, Copenhagen, 58 pp., ISBN 978-87-635-1258-9, 2002.

Saleh, G. M.: Rare metal-bearing pegmatites from the Southeastern Desert of Egypt: Geology, geochemical characteristics, and petrogenesis, Chinese J. Geochem., 26, 8–22, https://doi.org/10.1007/s11631-007-0008-8, 2007.

Schilling, J., Marks, M. W. A., Wenzel, T., Vennemann, T., Horváth, L., Tarassoff, P., Jacob, D. E., and Markl, G.: The magmatic to hydrothermal evolution of the intrusive Mont Saint-Hilaire Complex: insights into the late-stage evolution of peralkaline rocks, J. Petrol., 52, 2147–2185, https://doi.org/10.1093/petrology/egr042, 2011.

Schmid, S. M., Bernoulli, D., Fügenschuh, B., Matenco, L., Schefer, S., Schuster, R., Tischler, M., and Ustaszewski, K.: The Alpine-Carpathian-Dinaridic orogenic system - correlation and evolution of tectonic units, Swiss J. Geosci., 101, 139–183, https://doi.org/10.1007/s00015-008-1247-3, 2008.

Semenov, E. I.: Oxides and hydroxides of titanium and niobium in the Lovozero alkaline massif, Trudy Institutu mineralogii, geokhimii, i krystallokhimii redkikh elementov, 1, 41–59, 1957.

Sitnin, A. A. and Leonova, T. N.: Loparite – a new accessory mineral of albitized and greisenized granites, Dokl. Akad. Nauk SSSR, 140, 1407–1410, 1961.

Šmíd, B.: Výzkum vyvřelých hornin těšínitové asociace, PhD thesis, Ústřední ústav geologický, Praha, 153 pp., 1978.

Szopa, K., Włodyka, R., and Chew, D.: LA-ICP-MS U-Pb apatite dating of Lower Cretaceous rocks from teschenite-picrite association in the Silesian Unit (southern Poland), Geol. Carpath., 65, 273–284, https://doi.org/10.2478/geoca-2014-0018, 2014.

Tolok, A. A. and Bazhenova, F. V.: Loparite – a new accessory mineral of nepheline syenites of the Sikhote-Alin, Zapiski Vsesoyuznogo Mineralogicheskogo Obshchestva, 94, 217–219, 1965.

Tschernich, R. W.: Zeolites of the World, Geoscience Press, Phoenix, 563 pp., ISBN 0-945005-07-5, 1992.

Velde, B.: Clay minerals: A physio-chemical explanation of their occurrence, Developments in Sedimentology No. 40, Elsevier, Amsterdam – Oxford – New York – Tokyo, ISBN 978-0-444-42423-5, 1985.

Vlasov, K. A., Kuzmenko, M. Z., and Eskova, E. M.: The Lovozero alkali massif, Akademia Nauk SSSR/Hafner Publishing Company, New York, 627 pp., 1966.

Wilkinson, J. F. G. and Hensel, H. D.: Nephelines and analcimes in some alkaline igneous rocks, Contrib. Mineral. Petr., 118, 79–91, https://doi.org/10.1007/BF00310612, 1994.

Włodyka, R.: The evolution of mineral composition of the Cieszyn magma province rocks, Wydawnictwo Uniwersytetu Śląskiego, Katowice, 232 pp., ISBN 978-83-226-1894-3, 2010.

Yakovenchuk, V. N., Ivanyuk, G. Y., Pakhomovsky, Y. A., and Menshikov, Y. P.: Khibiny, Laplandia Minerals, Apatity, 466 pp., ISBN 5-900395-48-0, 2005.

Yan, S., Niu, H.-C., Zhao, X., Zhang, Q.-B., Zhang, H.-J., and Zhao, X.-C.: Rare metal enrichment of the Tianbao trachytic complex, North Daba Mountains (South Quinling): Insights from textures and geochemistry of trachytes and Nb-REE minerals, Ore Geol. Rev., 146, 104948, https://doi.org/10.1016/j.oregeorev.2022.104948, 2022.

Yaroshevskii, A. A. and Bagdasarov, Y. A.: Geochemical diversity of minerals of the pyrochlore group, Geochem. Int., 46, 1245–1266, https://doi.org/10.1134/S0016702908120045, 2008.

Zozulya, D., Kullerud, K., Ravna, E. K., Corfu, F., and Savchenko, Y.: Geology, age and geochemical constraints on the origin of the Late Archaean Mikkelvik alkaline stock, West Troms Basement Complex in Northern Norway, Norw. J. Geol., 89, 327–340, 2009.